

## Optimal Charge and Color Breaking conditions in the MSSM

C. Le Mouél<sup>1</sup>

Dept. of Theoretical Physics, Aristotle University of Thessaloniki,  
GR-54006 Thessaloniki, Greece.

Physique Mathématique et Théorique, UMR No 5825–CNRS,  
Université Montpellier II, F–34095 Montpellier Cedex 5, France.

### Abstract

In the Minimal Supersymmetric Standard Model, we make a careful tree-level study of Charge and Color Breaking conditions in the plane  $(H_2, \tilde{u}_L, \tilde{u}_R)$ , with particular attention paid to the large Yukawa coupling regime valid for the top quark case. A simple and fast procedure to compute the VEVs of the dangerous vacuum is presented and used to derive a model-independent optimal CCB bound on the trilinear soft term  $A_t$ . This bound takes into account all possible deviations of the CCB vacuum from the D-flat directions. For large  $\tan\beta$ , it provides a CCB maximal mixing for the stop scalar fields  $\tilde{t}_1, \tilde{t}_2$ , which automatically rules out the so-called Higgs maximal mixing  $|A_t| = \sqrt{6}m_{\tilde{q}}$ . As a result, strong model-independent limits are obtained on the stop mass spectrum and a substantial reduction on the one-loop upper bound of the lightest Higgs mass,  $m_h$ , can be obtained in some cases. In deriving such conclusions, the renormalization scale  $Q$  at which this tree-level optimal CCB condition is evaluated is chosen at an appropriate value in order to incorporate leading one-loop corrections.

---

<sup>1</sup>Electronic address: lemouel@physics.auth.gr

# 1 Introduction

Unlike the Standard Model (SM), the scalar sector of the Minimal Supersymmetric Standard Model (MSSM) [1] is extremely large and contains many scalar fields, some of them having non-trivial color and/or electric charges. The presence of such a large sector is dictated by supersymmetry (SUSY) [1, 2]. At the Fermi scale, global SUSY must however be broken and soft SUSY breaking terms which enter mostly in the scalar sector of MSSM distort the simple analytic structure of the SUSY effective potential and are responsible of a blowing-up of the number of free parameters in the MSSM [1, 2]. There are many ways to reduce to a great extent this huge number of parameters, further improving the predictivity of the MSSM. Each one relies on some particular scenario of SUSY breaking and mediation to the MSSM spectrum [3, 4]. Whatever such a model-dependent scenario may be, phenomenological consistency at the Fermi scale requires that spontaneous symmetry breaking of the SM gauge group should occur into the ElectroWeak (EW) vacuum, not in a color and/or electric charged vacuum. This Charge and Color Breaking (CCB) danger which does not exist in the SM was quickly realized in the MSSM [5], and has been extensively studied ever since [5, 6, 7, 8, 9, 10], providing useful complementary CCB conditions on the soft parameters.

The major difficulty in obtaining reliable CCB conditions comes from the extremely involved structure of the effective potential whose global minimum determines the vacuum of the theory. As a consequence, CCB studies concentrated on simple directions in the scalar field space, restricting also often to D-flat directions [5, 6, 7, 8, 9]. The last requirement simplifies greatly the analytical study of the minima of the potential and provides already rather strong CCB constraints which may in some cases rule out model-dependent scenarii [7] or, at least, severely constrain them [6, 7]. Another alternative is to handle the problem in a purely numerical way [8, 10], a rather blind method, time-consuming, which moreover faces the danger of missing CCB vacua because of the complexity of the potential.

Only but a few studies considered analytically, or semi-analytically, possible deviations of the CCB vacuum from D-flat directions. In ref.[6], in particular, it was shown that in the interesting field planes  $(H_1, H_2, \tilde{t}_L, \tilde{t}_R)$  and  $(H_1, H_2, \tilde{t}_L, \tilde{t}_R, \tilde{\nu}_L)$ , such deviations of the CCB vacuum typically occur, due essentially to large effects induced by the top Yukawa coupling [6]. To take into account this important feature, a semi-analytical procedure was proposed, and then illustrated in an mSUGRA context, giving refined CCB conditions in terms of the universal soft parameters at the GUT scale [6]. We stress however that model-dependent assumptions are implicitly present in this procedure, and need to be relaxed to get a fully satisfactory model-independent picture of CCB conditions. Furthermore, this procedure, somewhat, does not lend itself easily to the derivation of analytical expressions for the CCB Vacuum Expectation Values (VEVs) of the fields, and, hence, for the optimal conditions to avoid CCB. On the technical side, our purpose in this paper is to overcome these difficulties, though in the restricted plane  $(H_2, \tilde{t}_L, \tilde{t}_R)$ . This plane will actually provide us with a simplified framework where to present in detail an alternative procedure to evaluate the CCB VEVs. This way we will include in our study all possible deviations from the D-flat directions, and obtain an accurate analytical information on

them. This procedure can also be adapted to extended planes, and the present study will be followed by a complete investigation of CCB conditions in the planes  $(H_1, H_2, \tilde{t}_L, \tilde{t}_R)$  and  $(H_1, H_2, \tilde{t}_L, \tilde{t}_R, \tilde{\nu}_L)$  [11, 12].

More fundamentally, the plane  $(H_2, \tilde{t}_L, \tilde{t}_R)$  is also of particular interest for the following reasons:

**i)** The CCB vacuum typically deviates largely from the  $SU(2)_L \times U(1)_Y$  D-flat direction, as already observed in [6], but also from the  $SU(3)_c$  D-flat direction. The latter result, also shared by the potential in the extended planes  $(H_1, H_2, \tilde{t}_L, \tilde{t}_R)$  and  $(H_1, H_2, \tilde{t}_L, \tilde{t}_R, \tilde{\nu}_L)$  [11, 12], is in disagreement with the claim of [6]. As we will see, this important feature must be incorporated in order to obtain an optimal CCB condition which encompasses the requirement of avoiding a tachyonic lightest stop. We will give simple analytic criteria for alignment of the CCB vacuum in D-flat directions and show that alignment in the  $SU(3)_c$  D-flat direction is in fact a model-dependent statement which is approximately valid in an mSUGRA scenario [3], but not in other interesting models, e.g., some string-inspired or anomaly mediated scenarii [4].

**ii)** For large  $\tan \beta$ , the EW vacuum is located in the vicinity of the plane  $(H_2, \tilde{t}_L, \tilde{t}_R)$ . Therefore, in this regime, the study of this plane is self-sufficient: the free parameters entering the effective potential are enough to evaluate the optimal necessary and sufficient condition on  $A_t$  to avoid CCB. This does not mean that CCB conditions in the plane  $(H_2, \tilde{t}_L, \tilde{t}_R)$  are useless for low  $\tan \beta$ . We will give in this paper an analytic optimal sufficient condition to avoid CCB in this plane, and, to evaluate the complementary optimal necessary CCB condition, we will simply need some additional information on the depth of the EW potential, which reduces in fact to a particular choice for  $\tan \beta$  and the pseudo-scalar mass  $m_{A^0}$ .

Our purpose in this study is also to consider some physical consequences at the SUSY scale of the CCB conditions. We will investigate in detail the benchmark scenario  $M_{SUSY} = m_{\tilde{t}_L} = m_{\tilde{t}_R}$  and  $\tan \beta = +\infty$ , often considered in Higgs phenomenology [13, 14]. In this case, the stop mixing parameter equals the trilinear soft term,  $\tilde{A}_t \equiv A_t + \mu / \tan \beta = A_t$ . We will show that the so-called Higgs maximal mixing  $|A_t| = \sqrt{6}m_{\tilde{q}}$  is always largely ruled out by the optimal CCB condition. This will lead us to introduce a CCB maximal mixing, which induces strong bounds on the stop mass spectrum. Another direct implication of this result is a lowering of the one-loop upper bound on the CP-even lightest Higgs mass  $m_h$  reached for such a large  $\tan \beta$  regime [13, 14]. For illustration, this point will be considered in a simplified setting, where only top and stop contributions to  $m_h$  will be taken into account, assuming  $m_{A^0} \gg m_{Z^0}$ . This will already point out the importance of CCB conditions in this context, but should however be completed, to become more realistic, by a refined investigation including all one-loop and two loop contributions to  $m_h$  [13, 14]. In these illustrations, the leading one-loop corrections to the CCB condition will be incorporated by assuming that the tree-level CCB condition obtained are evaluated at an appropriate renormalization scale, estimated in fact to be the SUSY scale [6, 15]. This way, we expect the results presented in this paper to be robust under inclusion of such radiative corrections. Finally, we note that these results can be shown to be also numerically representative of the large  $\tan \beta$  regime with small enough values

of the supersymmetric term  $\mu$ , i.e.  $\tan \beta \gtrsim 15$  and  $|\mu| \lesssim \text{Min}[m_{A^0}, M_{SUSY}]$  [11].

**iii)** As is well-known, for metastability considerations, CCB vacua associated to the third generation of squarks are the most dangerous ones [9, 10, 16]. This comes from the fact that such vacua prove to be rather close to the EW vacuum, resulting in a barrier separating both vacua more transparent to a tunneling effect. We will see that combining experimental data on the lower bound of the lightest stop mass,  $m_{\tilde{t}_1}$ , with precise CCB conditions already delineates large regions in the parameter space where the EW vacuum is the deepest one and, hence, stable. Outside such regions, an optimal determination of the modified CCB metastable conditions requires first a precise knowledge of the geometrical properties of the effective potential, e.g., the positions of the CCB vacua and saddle-points. In this light, the analytical expressions presented in this article provide an essential information to investigate precisely metastability.

The paper is organized as follows. In section 2, we first review the issue of CCB conditions in the plane  $(H_2, \tilde{u}_L, \tilde{u}_R)$  in the D-flat direction. We turn then to the full plane case for the third generation of squark fields and give a first simple analytical sufficient condition on  $A_t$  to avoid CCB. In section 3, we detail our semi-analytical procedure to obtain the VEVs of the local extrema in this plane, discuss the deviation from the  $SU(3)_c$  D-flat, and give an optimal sufficient bound on  $A_t$  to avoid CCB. We discuss finally some geometrical features of the CCB vacuum. In section 4, we discuss the renormalization scale at which the tree-level CCB conditions obtained should be evaluated in order to incorporate leading one-loop corrections. In section 5, we summarize the practical steps needed to evaluate numerically the optimal necessary and sufficient CCB condition on  $A_t$ . Sections 6-7 are devoted to numerical illustrations and, for large  $\tan \beta$ , to phenomenological implications of the new optimal CCB condition for the stop mass spectrum and the one-loop upper bound on the lightest Higgs mass. Section 8 presents our conclusions. Finally, the appendices A and B contain some technical material and the generalization of this study to the plane  $(H_1, \tilde{b}_L, \tilde{b}_R)$ , valid for a large bottom Yukawa coupling, or equivalently for large  $\tan \beta$ .

## 2 CCB conditions in the plane $(H_2, \tilde{u}_L, \tilde{u}_R)$

We consider the tree-level effective potential in the plane  $(H_2, \tilde{u}_L, \tilde{u}_R)$ , where  $H_2$  denotes the neutral component of the corresponding Higgs scalar  $SU(2)_L$  doublet, and  $\tilde{u}_L, \tilde{u}_R$  are respectively the left and right up squark of the same generation. In this plane, the tree-level effective potential reads [5]

$$\begin{aligned} V_3 = & m_2^2 H_2^2 + m_{\tilde{u}_L}^2 \tilde{u}_L^2 + m_{\tilde{u}_R}^2 \tilde{u}_R^2 - 2Y_u A_u H_2 \tilde{u}_L \tilde{u}_R + Y_u^2 (H_2^2 \tilde{u}_L^2 + H_2^2 \tilde{u}_R^2 + \tilde{u}_L^2 \tilde{u}_R^2) \\ & + \frac{g_1^2}{8} (H_2^2 + \frac{\tilde{u}_L^2}{3} - \frac{4\tilde{u}_R^2}{3})^2 + \frac{g_2^2}{8} (H_2^2 - \tilde{u}_L^2)^2 + \frac{g_3^2}{6} (\tilde{u}_L^2 - \tilde{u}_R^2)^2 \end{aligned} \quad (1)$$

We suppose that all fields are real and that  $H_2, \tilde{u}_L$  are positive, which can be arranged by a phase redefinition. The Higgs mass parameter  $m_2^2 = m_{H_2}^2 + \mu^2$  can have both signs,  $m_{H_2}$  being the soft mass of the corresponding Higgs field;  $m_{\tilde{u}_L}^2, m_{\tilde{u}_R}^2$  are the squared soft

masses of the left and right up squarks and are supposed to be positive to avoid instability of the potential at the origin of the fields;  $Y_u$  and  $A_u$  stand for the Yukawa coupling and the trilinear soft coupling and are also supposed to be real and positive, which can be arranged once again by a phase redefinition of the fields; finally  $g_1, g_2, g_3$  are respectively the  $U(1)_Y, SU(2)_L, SU(3)_c$  gauge couplings.

## 2.1 The D-flat direction

In the D-flat direction  $|H_2| = |\tilde{u}_L| = |\tilde{u}_R|$ , the potential  $V_3$ , eq.(1), may develop a very deep CCB minimum, unless the well-known condition [5, 6]

$$A_u^2 \leq (A_{u,3}^D)^2 \equiv 3(m_{\tilde{u}_L}^2 + m_{\tilde{u}_R}^2 + m_2^2) \quad (2)$$

is verified. Strictly speaking, as the extremal equations easily show, the global minimum of the potential  $V_3$ , eq.(1), lies in the D-flat direction only for:

$$m_{\tilde{u}_L}^2 = m_{\tilde{u}_R}^2 = m_2^2 \quad (3)$$

However, *in the small Yukawa coupling regime*, valid for the first two generations of quarks, the VEVs of the CCB vacuum are large,  $\langle \phi \rangle \sim A_u/3Y_u$ . The vacuum then proves to be located in the vicinity of this direction [5, 6], even for large deviations from the mass relations in eq.(3). Moreover, due to the smallness of the Yukawa coupling, this CCB minimum is very deep,  $\langle V_3 \rangle \lesssim -A_u^2[A_u^2 - (A_{u,3}^D)^2]/27Y_u^2$ , and, with increasing  $A_u$ , gets rapidly<sup>1</sup> deeper than the realistic EW vacuum. As a result, the relation eq.(2) turns out to provide an accurate necessary and sufficient condition to avoid a CCB in this plane [5, 6].

*In the large Yukawa coupling regime*, valid for the top quark case, the condition eq.(2) is now only approximately necessary, because in some (small) range of values for  $A_t$  where it is not verified the CCB local minimum in the D-flat direction develops without being deeper than the EW vacuum. *It is however no more sufficient, the true global CCB minimum of  $V_3$ , eq.(1), being in general located far away from the D-flat direction* [6]! Obtaining the most accurate conditions to avoid CCB in the top quark regime needs to explore the scalar field space outside D-flat directions, a more difficult task which is of particular phenomenological interest, as we will see. In the following, we focus on this interesting regime in order to get a complete model-independent picture of CCB conditions in the plane  $(H_2, \tilde{t}_L, \tilde{t}_R)$ .

## 2.2 The full-plane case

Beyond a critical value for the trilinear soft term  $A_t$ , a dangerous CCB minimum, deeper than the EW vacuum, forms and deepens with increasing values of  $A_t$ . In ref.[6], it was advocated that such a global CCB minimum is located in general far away from

---

<sup>1</sup> Within less than 1 GeV.

the  $SU(2)_L \times U(1)_Y$  D-flat directions, but close to the  $SU(3)_c$  D-flat one. This work was performed in more extended planes with additional scalar fields,  $H_1$  and possibly a sneutrino field  $\tilde{\nu}_L$ , which we will consider in separate articles [11, 12]. Already in the plane  $(H_2, \tilde{t}_L, \tilde{t}_R)$ , our study indeed shows a typical large deviation of the CCB vacuum from the  $SU(2)_L \times U(1)_Y$  D-flat directions. However, in a model-independent way, we disagree with the claim of ref.[6] that the CCB vacuum always proves to be located in the vicinity of the  $SU(3)_c$  D-flat direction. Actually, alignment in this direction depends on the magnitude of the soft terms  $A_t, m_{\tilde{t}_L}, m_{\tilde{t}_R}$  [see sec.3.2] and occurs in two different circumstances: either i)  $m_{\tilde{t}_L} = m_{\tilde{t}_R}$ , or ii)  $A_t \gg m_{\tilde{t}_L}, m_{\tilde{t}_R}$ . Any discrepancy between the soft masses  $m_{\tilde{t}_L}, m_{\tilde{t}_R}$ , as happens for instance in some anomaly mediated models [4], is the source of a possibly large departure of the CCB vacuum from the  $SU(3)_c$  D-flat direction and, ultimately, of a sizeable enhancement of the optimal condition on  $A_t$  to avoid CCB. To consider this feature, we introduce a new parameter which conveniently measures the separation of the CCB extrema from the  $SU(3)_c$  D-flat direction

$$f \equiv \frac{\tilde{t}_R}{\tilde{t}_L} \quad (4)$$

Alignment in the  $SU(3)$  D-flat direction corresponds to  $\langle f \rangle = \pm 1$ .

We replace now  $\tilde{t}_R \rightarrow f \tilde{t}_L$  in  $V_3$ , eq.(1), which is unambiguous provided  $\tilde{t}_R \neq 0$ . By inspection of the extremal equation associated to the field  $\tilde{t}_L$ , it is easy to obtain a critical bound on  $A_t$  below which no CCB local minimum may exist. The non-trivial solution for the VEV  $\langle \tilde{t}_L \rangle$  verifies

$$A_3 < \tilde{t}_L \rangle^2 + 2B_3 = 0 \quad (5)$$

where  $A_3 \equiv g_1^2(4 \langle f \rangle^2 - 1)^2/18 + g_2^2/2 \langle f \rangle^4 + 2g_3^2(\langle f \rangle^2 - 1)^2/3 + 4Y_t^2 \langle f \rangle^2$ . This term is a sum of squared terms, therefore always positive. This implies the inequality

$$B_3 \equiv \langle H_2 \rangle^2 \frac{[(12Y_t^2 - 4g_1^2) \langle f \rangle^2 + 12Y_t^2 + g_1^2 - 3g_2^2]}{12} - 2A_t Y_t \langle f \rangle \langle H_2 \rangle + m_{\tilde{t}_L}^2 + \langle f \rangle^2 m_{\tilde{t}_R}^2 \leq 0 \quad (6)$$

$B_3$  may be considered as a polynomial in  $\langle H_2 \rangle$ . For  $Y_t \geq \text{Max}[\sqrt{(3g_2^2 - g_1^2)/12}, g_1/\sqrt{3}]$  the coefficient of the quadratic term in  $\langle H_2 \rangle$  is positive, whatever  $\langle f \rangle$ . At the EW scale, this relation reduces to  $Y_t \gtrsim 0.3$ , which anyway must be verified in order to have a correct top quark mass  $m_t \sim 175 \text{ GeV}$ . Obviously, the running of the parameters  $Y_t, g_1, g_2$  with respect to the renormalization scale will not alter this result, so that we can safely conclude that this coefficient is always positive. *Actually, this is precisely the turning point where the qualitative difference between the large and the small Yukawa coupling regimes enters the game.*

Keeping in mind this feature, eq.(6) implies that  $\langle f \rangle$  (and thus  $\langle \tilde{t}_R \rangle$ ) must be positive. The negativity of  $B_3$  requires in addition the positivity of the discriminant of  $B_3$  considered as a polynomial in  $\langle H_2 \rangle$ :

$$\begin{aligned} \Delta_{B_3} = & (m_{\tilde{t}_L}^2 + \langle f \rangle^2 m_{\tilde{t}_R}^2)[-4Y_t^2(\langle f \rangle^2 + 1) + \frac{g_1^2}{3}(4 \langle f \rangle^2 - 1) + g_2^2] \\ & + 4A_t^2 Y_t^2 \langle f \rangle^2 \geq 0 \end{aligned} \quad (7)$$

This inequality may be expressed as a condition on  $A_t$

$$A_t^2 \geq -\frac{(m_{\tilde{t}_L}^2 + \langle f \rangle^2 m_{\tilde{t}_R}^2)[-4Y_t^2(\langle f \rangle^2 + 1) + \frac{g_1^2}{3}(4\langle f \rangle^2 - 1) + g_2^2]}{4Y_t^2 \langle f \rangle^2} \quad (8)$$

The right hand side of this relation considered as a function of  $\langle f \rangle$  is bounded from below and gives an absolute lower bound on  $A_t$  below which  $\Delta_{B_3}$  can't be positive. This lower bound provides a first very simple sufficient condition to avoid any CCB minimum in the plane  $(H_2, \tilde{t}_L, \tilde{t}_R)$ :

$$A_t \leq A_t^{(0)} \equiv m_{\tilde{t}_L} \sqrt{1 - \frac{g_1^2}{3Y_t^2}} + m_{\tilde{t}_R} \sqrt{1 - \frac{(3g_2^2 - g_1^2)}{12Y_t^2}} \sim m_{\tilde{t}_L} + m_{\tilde{t}_R} \quad (9)$$

If this condition is verified, the global minimum of the potential  $V_3$ , eq.(1), is automatically trapped in the plane  $\tilde{t}_R = \tilde{t}_L = 0$  and cannot be lower than the EW vacuum.

Such a simple relation also sets a lower bound on  $A_t$  above which CCB may possibly occur and is already quite useful to secure some model-dependent scenarii. As a simple illustration, we consider the infrared quasi-fixed point scenario for low and large  $\tan \beta$ , in an mSUGRA context [17, 18]. For a top Yukawa coupling large enough at the GUT scale, the soft parameters  $m_{\tilde{t}_L}, m_{\tilde{t}_R}$  and  $A_t$  are strongly attracted in the infrared regime to quasi-fixed points. For  $\frac{Y_t}{g_i}|_{M_{GUT}} = 5$  and  $m_0 \lesssim m_{1/2}$ , where  $g_i$  stands for the three gauge couplings that unify at the GUT scale,  $M_{GUT}$ , and  $m_0, m_{1/2}$  are respectively the unified scalar and gaugino masses at the GUT scale, we have at one-loop level, in the infrared regime [18]:

$$m_{\tilde{t}_L}^2 \sim 0.70 M_3^2 \quad , \quad m_{\tilde{t}_R}^2 \sim 0.48 M_3^2 \quad \text{for low } \tan \beta \quad (10)$$

$$m_{\tilde{t}_L}^2 \sim 0.58 M_3^2 \quad , \quad m_{\tilde{t}_R}^2 \sim 0.52 M_3^2 \quad \text{for large } \tan \beta \quad (11)$$

giving  $A_t^{(0)} \sim 1.53 |M_3|$  ( for low  $\tan \beta$ ) and  $A_t^{(0)} \sim 1.48 |M_3|$  ( for large  $\tan \beta$ ), where  $M_3$  is the gluino mass. Comparing these bounds with the infrared quasi-fixed point value  $|A_t| \sim 0.62 |M_3|$  ( for both low and large  $\tan \beta$ ) [18], we see that the sufficient condition  $|A_t| \leq A_t^{(0)}$ , eq.(9), is largely fulfilled. Therefore, we conclude that the infrared quasi-fixed point scenario is free of CCB danger in the restricted plane  $(H_2, \tilde{t}_L, \tilde{t}_R)$ .

### 2.3 The critical CCB condition

In order to study the CCB extrema of the potential  $V_3$ , eq.(1), we suppose in the following that  $A_t > A_t^{(0)}$ . Consistency requires that, at any CCB extremum,  $\langle f \rangle$  and  $\langle H_2 \rangle$  are restricted to intervals which depend essentially on the soft breaking terms  $A_t, m_{\tilde{t}_L}, m_{\tilde{t}_R}$ : the positivity of  $\Delta_{B_3}$ , eq.(7), which may be viewed as a polynomial in  $\langle f \rangle^2$ , restricts  $\langle f \rangle$  in the interval given by the real and positive roots of  $\Delta_{B_3}$ ;  $\langle H_2 \rangle$  must be included between the real and positive roots of  $B_3$ , eq.(6). The potentially dangerous region of positive  $\langle \tilde{t}_L \rangle^2$  then proves to be located in a compact domain in the plane

$(H_2, f)$ , growing with  $A_t$ , with maximal extension

$$0 \leq \langle H_2 \rangle \leq \frac{6A_t Y_t}{\sqrt{(12Y_t^2 + g_1^2 - 3g_2^2)(3Y_t^2 - g_1^2)}} \lesssim \frac{A_t}{Y_t} \quad (12)$$

$$0 \leq \langle f \rangle \leq \frac{\sqrt{A_t^2 - m_{\tilde{t}_L}^2 (1 - g_1^2/3Y_t^2) - m_{\tilde{t}_R}^2 (1 - (3g_2^2 - g_1^2)/12Y_t^2)}}{m_{\tilde{t}_R} \sqrt{1 - g_1^2/3Y_t^2}} \lesssim \frac{A_t}{m_{\tilde{t}_R}} \quad (13)$$

Let us now replace in the potential  $V_3$ , eq.(1),  $\tilde{t}_L$  by the solution of eq.(5), and calculate the remaining two extremal equations. The derivative with respect to  $H_2$  provides an equation cubic in  $H_2$  and quartic in  $f$

$$\alpha_3 H_2^3 + \beta_3 H_2^2 + \gamma_3 H_2 + \delta_3 = 0 \quad (14)$$

with the coefficients

$$\begin{aligned} \alpha_3 = & -36Y_t^4(f^2 + 1)^2 + [3g_3^2(g_1^2 + g_2^2) + 4g_1^2 g_2^2](f^2 - 1)^2 \\ & + 6Y_t^2 g_1^2(4f^4 + 6f^2 - 1) + 18Y_t^2 g_2^2(2f^2 + 1) \end{aligned} \quad (15)$$

$$\beta_3 = 9A_t Y_t f[(12Y_t^2 - 4g_1^2)f^2 + 12Y_t^2 + g_1^2 - 3g_2^2] \quad (16)$$

$$\begin{aligned} \gamma_3 = & -72A_t^2 f^2 Y_t^2 - 3(m_{\tilde{t}_L}^2 + f^2 m_{\tilde{t}_R}^2)[(12Y_t^2 - 4g_1^2)f^2 + 12Y_t^2 + g_1^2 - 3g_2^2] \\ & + m_{\tilde{t}_L}^2[72Y_t^2 f^2 + g_1^2(4f^2 - 1)^2 + 9g_2^2 + 12g_3^2(f^2 - 1)^2] \end{aligned} \quad (17)$$

$$\delta_3 = 36A_t Y_t f(m_{\tilde{t}_L}^2 + f^2 m_{\tilde{t}_R}^2) \quad (18)$$

The derivative with respect to  $f$  provides an equation quadratic in  $H_2$  and quartic in  $f$

$$a_3 f H_2^2 + b_3 H_2 + c_3 f = 0 \quad (19)$$

with the coefficients

$$\begin{aligned} a_3 = & 2Y_t^2[(18Y_t^2 - 12g_3^2)(f^2 - 1) + 9g_2^2 - g_1^2(16f^2 - 1)] \\ & + (f^2 - 1)[4g_1^2 g_2^2 + 3(g_1^2 + g_2^2)g_3^2] \end{aligned} \quad (20)$$

$$b_3 = A_t Y_t [12g_3^2(f^4 - 1) - 9g_2^2 + g_1^2(16f^4 - 1)] \quad (21)$$

$$\begin{aligned} c_3 = & -m_{\tilde{t}_L}^2 [36Y_t^2 + 12g_3^2(f^2 - 1) + 4g_1^2(4f^2 - 1)] \\ & + m_{\tilde{t}_R}^2 [36f^2 Y_t^2 - 12g_3^2(f^2 - 1) + 9g_2^2 - g_1^2(4f^2 - 1)] \end{aligned} \quad (22)$$

A dangerous CCB minimum will have to verify the system of coupled equations eqs.(14,19), with the additional constraints that  $\langle H_2 \rangle, \langle f \rangle$  should be contained in the compact domain where  $\langle \tilde{t}_L \rangle^2 \geq 0$  [see eqs.(12, 13)].

To determine if such a CCB vacuum induces eventually a CCB situation, we need some additional information on the depth of the potential at a realistic EW vacuum. In the EW direction, the tree-level potential reads:

$$V|_{EW} = m_1^2 H_1^2 + m_2^2 H_2^2 - 2m_3^2 H_1 H_2 + \frac{(g_1^2 + g_2^2)}{8} (H_1^2 - H_2^2)^2 \quad (23)$$



where  $H_1$  denotes the neutral component of the corresponding Higgs scalar  $SU(2)_L$  doublet and is supposed to be real and positive, which can be arranged by a phase redefinition of the fields. Without loss of generality, we may also suppose that the Higgs mass parameters  $m_1^2, m_3^2$  are positive. The extremal equations in the EW direction read [1]:

$$\frac{m_1^2 - m_2^2 \tan^2 \beta}{\tan^2 \beta - 1} - \frac{m_{Z^0}^2}{2} = 0 \quad (24)$$

$$(m_1^2 + m_2^2)(1 + \tan^2 \beta) - 2m_3^2 \tan \beta = 0 \quad (25)$$

For  $\tan \beta \equiv v_2/v_1 \geq 1$ , where  $v_1, v_2$  are the VEVs of the EW vacuum, the minimal value of the EW potential is given by:

$$\langle V \rangle|_{EW} = -\frac{[m_2^2 - m_1^2 + \sqrt{(m_1^2 + m_2^2)^2 - 4m_3^4}]^2}{2(g_1^2 + g_2^2)} \quad (26)$$

The realistic EW vacuum is furthermore subject to the phenomenological constraint  $v_1^2 + v_2^2 = (174 \text{ GeV})^2$ , to reproduce correct masses for the gauge bosons  $Z^0, W^\pm$ . Experimental data also completely determine the gauge couplings  $g_1, g_2, g_3$ , and the top Yukawa coupling  $Y_t$ , the latter as a function of the physical top mass. Besides, we note that the depth of the EW potential  $\langle V \rangle|_{EW}$ , eq.(26), can be expressed with the help of the extremal equations eq.(24,25), as a function of  $\tan \beta$  and the pseudo-scalar mass  $m_{A^0} = \sqrt{m_1^2 + m_2^2}$ , which have a more transparent physical meaning. Moreover, we note that in order to incorporate leading one-loop contributions to the tree-level potential  $V|_{EW}$ , eq.(23), and therefore trust the results obtained with it up to one-loop level, the parameters should be evaluated at an appropriate renormalization scale  $Q \sim Q_{SUSY}$ , where this SUSY scale is an average of the typical SUSY masses at the EW vacuum [6, 15]. We will come back to this particular point in sec.4.

Comparison of the depth of the MSSM potential at the realistic EW vacuum and at the CCB vacuum induces in addition a new non-trivial relation with the three remaining free parameters  $A_t, m_{\tilde{t}_L}, m_{\tilde{t}_R}$  which enter the potential  $V_3$ , eq.(1). As a result, a critical bound  $A_{t,3}^c$  above which CCB occurs is identified:

$$CCB \Leftrightarrow \langle V_3 \rangle < \langle V \rangle|_{EW} \quad (27)$$

$$\Leftrightarrow A_t > A_{t,3}^c[m_{\tilde{t}_L}, m_{\tilde{t}_R}; m_1, m_2, m_3, Y_t, g_1, g_2, g_3] \quad (28)$$

We anticipate again on sec.4 and stress that this comparison of the depth of the tree-level potential at both vacua, and ultimately the value of the critical bound  $A_{t,3}^c$ , also incorporates leading one-loop contributions, provided all parameters are evaluated at the renormalization scale  $Q \sim Q_{SUSY}$ . To investigate this point and determine  $A_{t,3}^c$ , we need obviously a precise knowledge on the location and geometry of the CCB vacua. Sec. 3 is devoted to this particular topic. For a rapid overview of the situation the interested reader may also refer to sec.5 where we summarize some important points of this derivation and detail the practical steps to obtain the critical bound  $A_{t,3}^3$ .

### 3 The CCB vacuum in the plane $(H_2, \tilde{t}_L, \tilde{t}_R)$

#### 3.1 The algorithm to compute the CCB VEVs

To evaluate the CCB VEVs  $\langle H_2 \rangle$  and  $\langle f \rangle$ , a numerical step is now required. A numerical algorithm can be used for instance to solve simultaneously the two extremal equations eqs.(14,19). Such a method is however unable to bring any precise analytical information on the simple geometric behaviour of the CCB extrema of the potential  $V_3$ , eq.(1). Alternatively, we propose a procedure which has the good numerical properties of being fast, secure and easily implementable on a computer. Moreover, excellent analytical approximations for the CCB VEVs (at the level of the percent), and, ultimately, for the optimal conditions on  $A_t$  to avoid CCB can be obtained with it. Finally, it can be easily adapted to the extended planes  $(H_1, H_2, \tilde{t}_L, \tilde{t}_R)$  and  $(H_1, H_2, \tilde{t}_L, \tilde{t}_R, \tilde{\nu}_L)$ , first considered in [6], and this will enable us to shed new light on vacuum stability in these directions in a fully model-independent way [11, 12].

This alternative procedure to evaluate the CCB VEVs may be summarized as follows: we first insert an initial value  $f^{(0)}$  in the extremal equation associated to  $H_2$ , eq.(14). This equation is then solved in  $H_2$ . A solution  $H_2^{(0)}$ , which proves to be close to the CCB VEV  $\langle H_2 \rangle$ , is found. This solution is then inserted in the extremal equation associated to  $f$ , eq.(19), which is solved in  $f$ . We obtain an improved value  $f^{(1)}$ , closer to  $\langle f \rangle$  than  $f^{(0)}$ . The method is then iterated in a similar way. As a result, we obtain a set of numerical values  $(H_2^{(n)}, f^{(n)})_{n \geq 0}$  which proves to converge fast toward the true CCB extremal set  $(\langle H_2 \rangle, \langle f \rangle)$ .

More precisely, geometrical considerations confirmed by numerical analysis show that for a given set of free parameters  $A_t, m_{\tilde{t}_L}, m_{\tilde{t}_R}, \dots$  the potential  $V_3$ , eq.(1), may have only two non-trivial extrema with  $\langle \tilde{t}_{L,R} \rangle \neq 0$ : a CCB local minimum and a CCB saddle-point. Numerical analysis thus splits into two distinct branches, each one concerning one extremum. For simplicity, in this article we will not consider the behaviour of the CCB saddle-point solution, which is useful essentially for metastability considerations [9, 10]. Concerning the local CCB minimum, the apparent ambiguity in the implementation of the algorithm on the correct solutions  $(H_2^{(n)}, f^{(n)})$  to choose for each value of  $n \geq 0$  is easily lifted. As will be shown in sec.3.3, when a CCB minimum develops, the extremal equation associated to  $H_2$ , eq.(14) has necessarily three real positive roots in  $H_2$ . The correct solution  $(H_2^{(n)})_{n \geq 0}$  to follow is always the intermediate one. There is also no real ambiguity in the choice of  $(f^{(n)})_{n \geq 1}$ , because the extremal equation associated to  $f$ , eq.(19), has always only one real positive root in  $f$ , which is our candidate. Besides, the solutions of the extremal equation associated to  $H_2$ , eq.(14) [which gives the set of values  $(H_2^{(n)})_{n \geq 0}$ ], prove to vary very slowly as a function of  $f$ . This feature tends to boost the convergence of the procedure. Actually, starting with a clever choice for the input value  $f^{(0)}$ , the convergence is accelerated so that only one iteration is needed to fit the exact result with a precision of 1% or less, providing ultimately accurate analytical approximations for the CCB VEVs.

For completeness, let us briefly compare this method to evaluate the VEVs with the

one presented in ref.[6]. Assuming alignment of the CCB vacuum in the  $SU(3)_c$  D-flat direction, as done in [6], i.e.  $\langle f \rangle = 1$ , we obtain easily analytical expressions for the CCB VEVs depending only on the free parameters  $A_t, m_{\tilde{t}_L}, m_{\tilde{t}_R}, \dots$ , whereas with the method presented in [6] a numerical scan is still required: taking  $f^{(0)} = \langle f \rangle = 1$ , the VEV  $\langle H_2 \rangle$  is simply obtained with our method by solving analytically the cubic extremal equation eq.(14); the squark fields VEVs  $\langle \tilde{t}_L \rangle = \langle \tilde{t}_R \rangle$  are finally obtained by eq.(5). In addition, our iterative algorithm enables us to take into account, with any desired accuracy, any deviation of the CCB vacuum from the  $SU(3)_c$  D-flat direction. As noted before, in a model-independent way, such a deviation typically occurs. This point will be investigated more attentively in the next section, sec.3.2, by considering the extremal equation associated to  $f$ , eq.(19). A subsequent study of the extremal equation associated to  $H_2$ , eq.(14), will also provide us with a model-independent optimal bound on  $A_t$ , above which a local CCB vacuum begins to develop in the plane  $(H_2, \tilde{t}_L, \tilde{t}_R)$ . This point will be addressed in sec.3.3.

### 3.2 The deviation from the $SU(3)_c$ D-flat direction

We consider now deviations of the CCB vacuum from the  $SU(3)_c$  D-flat direction. In ref.[6], it was argued that, in a model-independent way, the CCB vacuum is located very close to this D-flat direction. As noted before, we disagree with this statement and show in this section that this assumption is model-dependent. Actually, such a deviation can be quite large, in particular for large discrepancies between the soft squark masses  $m_{\tilde{t}_L}, m_{\tilde{t}_R}$ , and results in a substantial enhancement of the necessary and sufficient condition to avoid CCB,  $A_t \leq A_{t,3}^c$ , eq.(27). In fact, the critical bound  $A_{t,3}^c$  can be shown to become more restrictive and this feature is essential, on a phenomenological ground, when it comes to relate CCB conditions with the requirement of avoiding a tachyonic lightest stop. As is well-known, a too large trilinear soft term  $A_t$  can increase this danger, but also any discrepancy  $m_{\tilde{t}_L} \neq m_{\tilde{t}_R}$ . The latter effect can be compensated only by taking into account the deviation of the CCB vacuum from the  $SU(3)_c$  D-flat direction.

The parameter controlling the deviation of the CCB vacuum from the  $SU(3)_c$  D-flat direction is the VEV  $\langle f \rangle$ . In the framework of our algorithm to compute the CCB VEVs, an educated guess for the initial value  $f^{(0)}$  should incorporate information on the extremal equation associated to  $f$ , eq.(19). Numerical analysis shows that, to an excellent accuracy,  $\langle f \rangle$  is related to  $\langle H_2 \rangle$  by the relation

$$\langle f \rangle \sim \bar{f}(\langle H_2 \rangle) \equiv \sqrt{\frac{m_{\tilde{t}_L}^2 + Y_t^2 \langle H_2 \rangle^2}{m_{\tilde{t}_R}^2 + Y_t^2 \langle H_2 \rangle^2}} \quad (29)$$

If we neglect gauge contributions,  $\bar{f}(H_2)$  is actually the exact solution to eq.(19). Therefore, this numerical observation simply reflects the fact that the deviation of the CCB vacuum from the  $SU(3)_c$  D-flat direction is nearly independent of the D-terms contributions in the potential  $V_3$ , eq.(1).

To go further, we need to approximate  $\langle H_2 \rangle$ . We note first that  $\bar{f}(H_2)$  is a slowly varying function of  $H_2$ , so that this approximation does not need to be very accurate. Neglecting in the potential  $V_3$ , eq.(1), the contributions of the gauge terms and

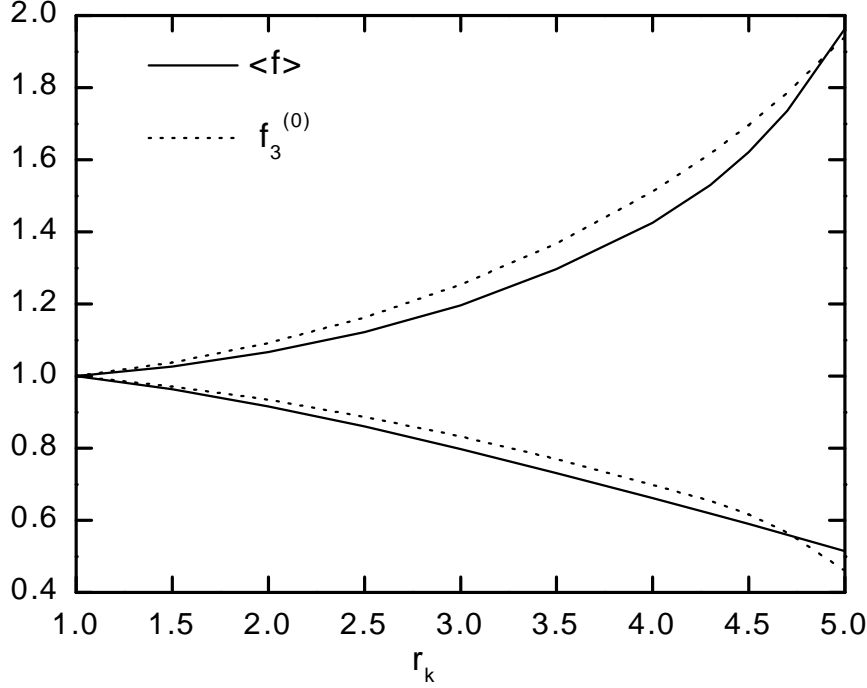


Figure 1:  $\langle f \rangle$ ,  $f_3^{(0)}$  versus  $r_k \equiv (m_{\tilde{t}_L}/m_{\tilde{t}_R})^k$ , for  $k = 1$ ,  $m_{\tilde{t}_R} = 200 \text{ GeV}$  (upper curves) and  $k = -1$ ,  $m_{\tilde{t}_L} = 200 \text{ GeV}$  (lower curves). We take  $A_t = 1400 \text{ GeV}$ ,  $m_2 = 118 \text{ GeV}$ ,  $Y_t = 1.005$ ,  $g_1 = 0.356$ ,  $g_2 = 0.649$ ,  $g_3 = 1.14$ .

the Higgs mass term  $m_2^2$ , and writing the potential as a function of  $B_3$ , eq.(6), we find  $V_3 \sim -B_3^2/(16Y_t^2 f^2)$ . This simple expression shows that a rough estimate of the VEV  $\langle H_2 \rangle$  is given by the minimal value taken by  $B_3$ , eq.(6):

$$\langle H_2 \rangle \sim \frac{A_t}{Y_t} \frac{\langle f \rangle}{(1 + \langle f \rangle^2)} \quad (30)$$

In fact, the exact VEV  $\langle H_2 \rangle$  is numerically typically found to be lower than this approximate value, but the latter already contains useful enough information for our purpose. Taking this value and solving  $\langle f \rangle = \bar{f}(\langle H_2 \rangle)$ , we obtain in turn the excellent approximation to  $\langle f \rangle$

$$\langle f \rangle \sim f_3^{(0)} \equiv \sqrt{\frac{A_t^2 + 2m_{\tilde{t}_L}^2 - m_{\tilde{t}_R}^2}{A_t^2 + 2m_{\tilde{t}_R}^2 - m_{\tilde{t}_L}^2}} \quad (31)$$

This approximate value  $f_3^{(0)}$  is equal to 1 (alignment in the  $SU(3)_c$  D-flat direction) for  $m_{\tilde{t}_L}^2 = m_{\tilde{t}_R}^2$ . This correctly reproduces the expected behaviour for  $\langle f \rangle$ : when the mass relation  $m_{\tilde{t}_L}^2 = m_{\tilde{t}_R}^2$  holds, the potential  $V_3$ , eq.(1), has an underlying approximate symmetry  $\tilde{t}_L \leftrightarrow \tilde{t}_R$  broken by tiny  $O(g_1^2, g_2^2)$  contributions, so that any non-trivial extremum must be nearly aligned in the  $SU(3)_c$  D-flat direction. In the large  $A_t$  regime, we have also  $f_3^{(0)} \rightarrow 1$ , reproducing again the expected behaviour for  $\langle f \rangle$ . Quite similarly to the small Yukawa coupling regime, in this limit, the VEVs of the CCB vacuum become very large. The vacuum then moves towards the  $SU(3)_c \times SU(2)_L \times U(1)_Y$  D-flat direction,

any splitting between the soft squark masses becoming inessential.

In Figure 1, we illustrate the evolution of the exact VEV  $\langle f \rangle$  and the approximation  $f_3^{(0)}$ , eq.(31), as a function of the ratio of the soft squark masses  $r_k \equiv (m_{\tilde{t}_L}/m_{\tilde{t}_R})^k$  for two cases  $k = \pm 1$ . The exact VEV  $\langle f \rangle$  has been computed with the recursive algorithm presented above [see also sec.5 for a practical summary], taking for initial value  $f^{(0)} = f_3^{(0)}$ , eq.(31). In both cases, we have taken  $A_t = 1400 \text{ GeV}$ . This implies in particular that the expression  $f_3^{(0)}$ , eq.(31), is defined up to  $r_k \sim 7.14$ . However, this approximation is appropriate only if a CCB vacuum exists. The sufficient bound given by eq.(9) already shows that a CCB vacuum can develop only for  $r_k \leq 6$ . Once optimized, the sufficient bound to avoid CCB restricts even more the allowed range to  $r_k \lesssim 5.3$  [see e.g. eq.(36) in sec.3.3]. In Fig.1, the evolution of the VEV is stopped at the boundary value  $r_k \sim 5$ , because the CCB vacuum becomes dangerous and deeper than the EW vacuum only below this value.

The first prominent feature of this illustration is that  $f_3^{(0)}$  is an excellent approximation:  $f_3^{(0)}$  fits  $\langle f \rangle$  with a precision of order 5%, or even better in the vicinity of  $r_k \sim 1$ . Moreover, we note that for a large splitting of the soft squark masses, the deviation of the CCB global minimum from the  $SU(3)_c$  D-flat direction can be quite large, in particular in the vicinity of the critical bound  $A_{t,3}^c$ , i.e. for  $r_k \sim 5$ . It is smaller for  $r_k \sim 1$ , where the CCB vacuum is nearly aligned in the  $SU(3)_c$  D-flat direction.

Finally, we may derive refined bounds on the deviation of the CCB vacuum from the  $SU(3)_c$  D-flat direction by combining the sufficient bound  $A_t^{(0)}$ , eq.(9), with the accurate approximation  $f_3^{(0)}$ , eq.(31). Requiring  $A_t \geq A_t^{(0)} \sim m_{\tilde{t}_L}(1 + r_1)$ , we obtain:

$$\text{For } r_1 \equiv \frac{m_{\tilde{t}_L}}{m_{\tilde{t}_R}} \geq 1, \quad 1 \leq \langle f \rangle \sim f_3^{(0)} \lesssim \sqrt{\frac{r_1(3r_1 + 2)}{2r_1 + 3}} \quad (32)$$

For  $r_1 \leq 1$  these inequalities are reversed.

In an mSUGRA scenario [3, 19], we fall typically in the regime  $r_1 \geq 1$ , with furthermore  $r_1$  perturbatively close to 1. Eq.(32) then implies  $1 \leq \langle f \rangle \lesssim 1 + \frac{3}{5}(r_1 - 1)$ , showing that the CCB vacuum is indeed located in the vicinity of the  $SU(3)_c$  D-flat direction. Such a feature was built-in through the procedure proposed to evaluate the CCB conditions in ref.[6], quite consistently with the mSUGRA numerical illustration presented in this article. However, it is important to stress that this assumption is model-dependent, and may be badly violated in other circumstances near the critical value  $A_{t,3}^c$ , in particular in scenarii incorporating non-universalities of the soft squark masses where the splitting parameter  $r_1$  can be rather large [4].

### 3.3 The optimal sufficient bound on $A_t$ to avoid CCB

We consider now more attentively the extremal equation associated to  $H_2$ , eq.(14). This complementary equation will in fact enable us to improve the sufficient bound  $A_t^{(0)}$ , eq.(9), to avoid a dangerous CCB vacuum in the plane  $(H_2, \tilde{t}_L, \tilde{t}_R)$ . From a geometrical point of view, it is reasonable to define the optimal sufficient CCB bound on  $A_t$  to be the largest value below which a local CCB minimum, not necessarily global, cannot develop.

Equivalently, this bound, denoted  $A_t^{suf}$  in the following, is also the critical value above which a local CCB vacuum begins to develop in the plane  $(H_2, \tilde{t}_L, \tilde{t}_R)$ .

The determination of the optimal sufficient bound  $A_t^{suf}$  simply requires some additional pieces of information on the extremal equation associated to  $H_2$ , eq.(14), and on the geometry of potential  $V_3$ , eq.(1). In order not to surcharge the text, we will not enter here in the details of this derivation, but rather refer the reader to the Appendix A. To summarize, on the technical side, the essential result we obtain is that if the extremal equation, eq.(14), considered as a cubic polynomial in  $H_2$ , has only one real root in  $H_2$  for any given value of  $f$ , then necessarily no local CCB minimum in the plane  $(H_2, \tilde{t}_L, \tilde{t}_R)$  can develop. More intuitively, this result merely reflects the fact that if a local CCB vacuum develops with non trivial VEVs ( $\langle H_2 \rangle, \langle f \rangle$ ), then on any path connecting the local extremum at the origin of the fields to this CCB vacuum, there will be necessarily a saddle on the top of the barrier separating them, with  $\tilde{t}_R, \tilde{t}_L \neq 0$ . For  $f = \langle f \rangle$ , such a point will in turn necessarily correspond to a second real solution in  $H_2$  for the extremal equation, eq.(14), in contradiction with the initial assumption.

Considering the extremal equation eq.(14) as a cubic polynomial in  $H_2$ , a necessary and sufficient condition to have only one real root is

$$\mathcal{C}_3 \equiv [\beta_3^3 - 9\alpha_3\beta_3\gamma_3 + 27\alpha_3^2\delta_3]^2 + 4[-\beta_3^2 + 3\alpha_3\gamma_3]^3 \geq 0 \quad (33)$$

The next step to evaluate the optimal sufficient bound  $A_t^{suf}$  is to consider this complicated inequality in the direction of a possible CCB minimum  $f = \langle f \rangle$ . Taking instead the approximate value  $f \sim f_3^{(0)}$ , given by eq.(31), and taking also values for all the parameters except the trilinear soft term  $A_t$ , the equation  $\mathcal{C}_3 = 0$  may be solved numerically as a function of  $A_t$ <sup>2</sup>. Let us denote  $A_t^{(1)}$  the largest solution of this equation. For  $A_t \leq A_t^{(1)}$ , we find numerically that we always have  $\mathcal{C}_3 \geq 0$ , showing that there can be no CCB vacuum in this case. Moreover, numerical investigation also shows that  $A_t^{(1)}$  has typically the desired property of being larger than  $A_t^{(0)}$ , eq.(9), and, therefore, improves this bound. There is only one exception to this statement, which occurs for  $m_2^2 \leq 0$  and  $m_{\tilde{t}_L}, m_{\tilde{t}_R} \sim m_t$ . As will be explained in the next section sec.3.4, this regime actually corresponds to a rather particular situation where no dangerous CCB vacuum deeper than the EW vacuum may develop, unless the EW vacuum is unstable.

Taking into account this observation, numerical investigation finally shows that for  $A_t \geq \text{Max}[A_t^{(0)}, A_t^{(1)}]$ , a local CCB vacuum begins to develop in the plane  $(H_2, \tilde{t}_L, \tilde{t}_R)$ . Hence, this critical value fulfills the properties required to be identified with the optimal sufficient bound  $A_t^{suf}$ . In conclusion, we may write without loss of generality:

$$A_t \leq A_t^{suf} \equiv \text{Max}[A_t^{(0)}, A_t^{(1)}] \Leftrightarrow \text{No local CCB vacuum} \quad (34)$$

where  $A_t^{(0)}$  is given by eq.(9) and  $A_t^{(1)}$  is obtained by solving  $\mathcal{C}_3 = 0$ , eq.(33), as mentioned above. It is important to stress here that this optimal sufficient bound, obtained with exact analytical expressions, incorporates all possible deviations of the CCB local vacuum

---

<sup>2</sup>Comparing with a more accurate value for  $\langle f \rangle$ , we found that the maximal discrepancy between the results obtained is negligible, less than 1 GeV.

from the D-flat directions, including the  $SU(3)_c$  D-flat one.

As  $A_t$  increases above  $A_t^{suf}$ , the CCB local vacuum soon becomes global and deeper than the EW vacuum. Obviously, the critical bound  $A_{t,3}^c$ , eq.(27), is necessarily larger than  $A_t^{suf}$ :

$$A_{t,3}^c \geq A_t^{suf} \quad (35)$$

Moreover, we expect that the critical bound  $A_{t,3}^c$  should be perturbatively close to the optimal sufficient bound  $A_t^{suf}$ , i.e.  $A_{t,3}^c \gtrsim A_t^{suf}$ , because the EW potential is not very deep,  $\langle V \rangle_{EW} \sim -m_Z^4/(g_1^2 + g_2^2)$ . Indeed, as will be illustrated in sec.5, the critical bound  $A_{t,3}^c$  is typically located in a range of 5% or less above  $A_t^{suf}$ . This interesting feature will considerably simplify the exact determination of  $A_{t,3}^c$ , which will be simply obtained by scanning a small interval in  $A_t$  above  $A_t^{suf}$ . We note finally that in the interesting phenomenological regime  $m_{\tilde{t}_L}, m_{\tilde{t}_R} \gtrsim 300 \text{ GeV}$ , a simple empirical approximation of  $A_t^{suf}$  may be obtained numerically. We find on one hand  $A_t^{suf} = A_t^{(1)}$ , with furthermore:

$$A_t^{suf} = A_t^{(1)} \sim A_t^{ap} \equiv m_{\tilde{t}_L} + m_{\tilde{t}_R} + |m_2| \quad (36)$$

This approximation exhibits in which amount the sufficient bound  $A_t^{(0)}$  is improved in this regime. The difference is of order  $|m_2|$ :  $A_t^{(1)} - A_t^{(0)} \sim |m_2|$ .

Let us come back briefly now to the implementation of the procedure to compute the CCB VEVs. We have shown that for  $A_t \leq A_t^{suf}$ , eq.(34), no local CCB vacuum may develop in the plane  $(H_2, \tilde{t}_L, \tilde{t}_R)$ . As noted before, in the dangerous complementary regime,  $A_t \geq A_t^{suf}$ , we need to evaluate the VEVs of the CCB local vacuum in order to compare the depth of the CCB potential and the EW potential and find the necessary and sufficient bound  $A_{t,3}^c$ , eq.(27), to avoid CCB. For  $f = f_3^{(0)}$ , eq.(31), the extremal equation associated to  $H_2$ , eq.(14), has three real roots, which also prove to be positive [see Appendix A]. The intermediate root, denoted  $H_2^{(0)}$  in sec.3.1, proves to be an excellent approximation of the VEV  $\langle H_2 \rangle$  [at a level of  $\lesssim 1\%$ ]<sup>3</sup>. The analytic expression of  $H_2^{(0)}$  is complicated and not particularly telling, therefore we refrain from giving it here. This shows that, to an excellent approximation, we can obtain explicit analytic expressions for all the CCB VEVs:  $(\langle H_2 \rangle, \langle f \rangle)$  are approximated by  $(H_2^{(0)}, f_3^{(0)})$ , where  $f_3^{(0)}$  enables us to take into account the deviation of the CCB vacuum from the  $SU(3)_c$  D-flat direction, and the squark VEVs  $\langle \tilde{t}_{L/R} \rangle$  are subsequently obtained by eqs.(4,5). This way, we can obtain in turn an accurate analytical expression for the CCB potential  $V_3$ , eq.(1), at the CCB vacuum. Comparison with the EW potential  $\langle V \rangle_{EW}$ , eq.(26), ultimately provides an excellent approximation of the critical CCB bound  $A_{t,3}^c$ , eq.(27). The accuracy of this approximation can be improved at will by iterating the procedure to compute the CCB VEVs, as depicted in sec.3.1. We note however that the impact on  $A_{t,3}^c$  is negligible,  $\sim O(1 \text{ GeV})$ .

---

<sup>3</sup>For completeness, we note that typically the lowest solution will correspond to a directional CCB saddle-point, whereas the largest is spurious, giving  $\langle \tilde{t}_L \rangle^2 \leq 0$

### 3.4 The instability condition of the EW potential

Besides the contribution of the trilinear soft term  $A_t$ , another negative contribution in the potential  $V_3$ , eq.(1), appears at the EW scale when the Higgs parameter  $m_2^2$  becomes negative. At the tree-level, the sign of  $m_2^2$  is related in a simple way to  $\tan\beta$  by the extremal equation eq.(25) in the EW direction: for  $\tan\beta \geq \sqrt{1 + 2m_{A^0}^2/m_{Z^0}^2}$ ,  $m_2^2$  is negative, whereas it is positive in the complementary low  $\tan\beta$  regime. Numerical investigation shows that we have only two distinct patterns for the number of local extrema of  $V_3$ , eq.(1). They are distinguished by the sign of  $m_2^2$  and, consequently, the magnitude of  $\tan\beta$ .

- $m_2^2 \geq 0$  :

The potential  $V_3$ , eq.(1), has one trivial local minimum, namely the origin of the field, and possibly a pair of non-trivial local extrema with  $\langle \tilde{t}_{L,R} \rangle \neq 0$ : the would-be global CCB vacuum and a CCB saddle-point sitting on top of the barrier separating it from the origin of the fields. In this case, the optimal sufficient bound  $A_t^{suf}$ , eq.(34), always prove to be equal to  $A_t^{(1)}$ . Besides, for soft squark masses large enough, i.e.  $m_{\tilde{t}_L}, m_{\tilde{t}_R} \gtrsim |m_2|$ , the traditional CCB bound in the D-flat direction  $A_{t,3}^D$ , eq.(2), typically provides an upper bound for the critical bound  $A_{t,3}^c$ , eq.(27), so that we may write:

$$A_t^{suf} = A_t^{(1)} \leq A_{t,3}^c \leq A_{t,3}^D \quad (37)$$

We note however that this upper bound is not very indicative of the critical value  $A_{t,3}^c$  for large values of the soft masses,  $m_{\tilde{t}_L}, m_{\tilde{t}_R} \gg |m_2|$ , as will be illustrated in sec.5. Actually, in this regime, the relation eq.(3) which is the signature of an alignment in the D-flat direction is badly violated, implying a large deviation of the CCB vacuum from the D-flat direction.

- $m_2^2 \leq 0$  :

Besides the origin of the fields and possibly a pair of CCB extrema (a local minimum and a saddle-point), the potential  $V_3$ , eq.(1), has another non-trivial extremum with VEVs  $\langle H_2 \rangle_{EW}^2 = -4m_2^2/(g_1^2 + g_2^2)$ ,  $\langle \tilde{t}_{R,L} \rangle_{EW} = 0$ , giving  $\langle V_3 \rangle_{EW} = -2m_2^4/(g_1^2 + g_2^2)$ . The origin of the fields is now unstable and the potential automatically bends down in the direction of this non-CCB extremum. We note also that, for large  $\tan\beta$ , the EW vacuum tends towards it as the inverse power of  $\tan\beta$ :  $(v_1 = (174\text{GeV})/\sqrt{1 + \tan^2\beta}, v_2) \rightarrow (0, \langle H_2 \rangle_{EW})$ . [Accordingly, the negativity of  $m_2^2$  appears as a mark in the plane  $(H_2, \tilde{t}_L, \tilde{t}_R)$  of the well-known instability condition at the origin of the fields  $m_1^2 m_2^2 - m_3^4 \leq 0$ , which is the signal an EW symmetry breaking [1]].

Obviously, if this additional extremum is a saddle-point of the potential  $V_3$ , eq.(1), then a deeper CCB minimum is necessarily present in the plane  $(H_2, \tilde{t}_L, \tilde{t}_R)$ . The squared mass



matrix evaluated at the non-CCB extremum reads

$$\mathcal{M}^2|_{\overline{EW}} = \begin{pmatrix} \frac{g_1^2 + g_2^2}{2} H_2^2 & 0 & 0 \\ 0 & m_{\tilde{t}_L}^2 + Y_t^2 H_2^2 (1 - \frac{(3g_2^2 - g_1^2)}{12Y_t^2}) & -A_t Y_t H_2 \\ 0 & -A_t Y_t H_2 & m_{\tilde{t}_R}^2 + Y_t^2 H_2^2 (1 - \frac{g_1^2}{3Y_t^2}) \end{pmatrix} \quad (38)$$

with  $H_2 = \langle H_2 \rangle_{\overline{EW}}$ .

Stability of the non-CCB vacuum is equivalent to the positivity of all the squared mass eigenvalues of  $\mathcal{M}^2|_{\overline{EW}}$ , eq.(38). It is not automatic and needs

$$A_t \leq A_t^{inst} \quad (39)$$

where

$$\begin{aligned} (A_t^{inst})^2 &\equiv m_{\tilde{t}_L}^2 (1 - \frac{g_1^2}{3Y_t^2}) + m_{\tilde{t}_R}^2 (1 - \frac{(3g_2^2 - g_1^2)}{12Y_t^2}) - \frac{g_1^2 + g_2^2}{4m_2^2} \frac{m_{\tilde{t}_L}^2 m_{\tilde{t}_R}^2}{Y_t^2} \\ &\quad - \frac{4m_2^2}{g_1^2 + g_2^2} Y_t^2 (1 - \frac{(3g_2^2 - g_1^2)}{12Y_t^2}) (1 - \frac{g_1^2}{3Y_t^2}) \end{aligned} \quad (40)$$

Let us remark that, for  $\tan \beta \rightarrow +\infty$ , the lower  $2 \times 2$  matrix of  $\mathcal{M}^2|_{\overline{EW}}$ , eq.(38), is simply equal to the tree-level physical squared stop mass matrix [1], so that the instability condition, eq.(39), is a mere rephrasing of the physical requirement of avoiding a tachyonic lightest stop, expressed as a function of  $A_t$ . This statement is also valid to a good accuracy when the stop mixing parameter  $\tilde{A}_t = A_t + \mu/\tan \beta$  is well approximated by the trilinear soft term  $A_t$ , i.e. for  $|\mu| \ll |A_t| \tan \beta$ .

To simplify the discussion, in the following we will essentially identify this non-CCB extremum with the EW vacuum, implying in particular that the potential at both vacua are equal, i.e.  $\langle V \rangle|_{EW} \sim \langle V_3 \rangle_{\overline{EW}}$ . This assumption, accurate for  $\tan \beta$  large enough, enables us to write the following relation on the CCB bounds

$$A_t^{suf} \leq A_{t,3}^c \leq A_t^{inst} \quad (41)$$

The first relation was actually obtained in the last section, see eq.(35), whereas the second means that if the non-CCB extremum is unstable, then a dangerous CCB vacuum, deeper than the EW vacuum<sup>4</sup>, has developed in the plane  $(H_2, \tilde{t}_L, \tilde{t}_R)$ .

For  $m_2^2 \leq 0$ , the relation (41) provides the most general upper and lower bounds on the critical CCB bound  $A_{t,3}^c$ , eq.(27). We note however that in the interesting regime of large squark soft masses, i.e.  $m_{\tilde{t}_L}, m_{\tilde{t}_R} \geq m_t$ , the upper bound given by  $A_t^{inst}$  is typically largely improved by the traditional bound in the D-flat direction  $A_{t,3}^D$ , eq.(2). However, quite similarly to the case  $m_2^2 \geq 0$ , the latter bound  $A_{t,3}^D$  is itself typically very large compared to

---

<sup>4</sup>The relation  $A_{t,3}^c \leq A_t^{inst}$  is still accurate if we relax our simplifying assumption  $\langle V \rangle|_{EW} \sim \langle V_3 \rangle_{\overline{EW}}$ , because the potential  $V_3$  deepens rapidly with increasing  $A_t$ .

the critical CCB bound  $A_{t,3}^c$ , due to a large deviation of the CCB vacuum from the D-flat directions. A better indication of the critical CCB bound  $A_{t,3}^c$ , eq.(27), is always given by the optimal sufficient bound  $A_t^{suf}$ , eq.(34).

Finally, let us consider more attentively the behaviour of the potential in the limit  $A_t \rightarrow A_t^{inst}$ . This will enlighten the importance of taking into account any deviation of CCB vacuum from the  $SU(3)_c$  D-flat direction in order to obtain a consistent critical CCB bound  $A_{t,3}^c$ , eq.(27), which encompasses the possibility of avoiding a tachyonic stop mass. Two interesting different modes with particular geometrical features of the potential can be considered:

- i) The CCB vacuum is located away from the non-CCB extremum. This possibility in fact corresponds either to the case  $m_{\tilde{t}_L} m_{\tilde{t}_R} \ll m_t^2$  or  $m_{\tilde{t}_L} m_{\tilde{t}_R} \gg m_t^2$ , where  $m_t$  is the top quark mass. In the first case, the CCB vacuum proves to be closer to the origin of the fields than the non-CCB extremum, whereas in the latter this hierarchy is reversed. In both cases, the optimal sufficient bound  $A_t^{suf}$ , eq.(34), is always given by  $A_t^{(1)}$ . In the limit  $A_t \rightarrow A_t^{inst}$ , the CCB saddle-point located on top of the barrier separating the CCB vacuum and the non-CCB extremum tends towards the non-CCB extremum and the barrier separating both vacua eventually disappears.
- ii) The CCB vacuum interferes with the non-CCB vacuum. For  $A_t \rightarrow A_t^{inst}$ , this mode corresponds to a degenerate situation where the CCB local vacuum and the CCB saddle-point overlap and tend towards the non-CCB vacuum. This possibility appears clearly by comparing the instability bound  $A_t^{inst}$ , eq.(39), with the sufficient bound  $A_t^{(0)}$ , eq.(9). We have

$$(A_t^{inst})^2 - (A_t^{(0)})^2 = [m_{\tilde{t}_L} m_{\tilde{t}_R} - (1 - \frac{(3g_2^2 - g_1^2)}{12Y_t^2})(1 - \frac{g_1^2}{3Y_t^2})Y_t^2 H_2^2]^2 \frac{1}{Y_t^2 H_2^2} \geq 0 \quad (42)$$

with  $H_2 = < H_2 >_{EW}$ . Combining the last equation with eq.(41), we obtain:

$$m_{\tilde{t}_L} m_{\tilde{t}_R} = [1 - \frac{(3g_2^2 - g_1^2)}{12Y_t^2}][1 - \frac{g_1^2}{3Y_t^2}] m_t^2 \Leftrightarrow A_{t,3}^c = A_t^{inst} = A_t^{suf} [= A_t^{(0)}] \quad (43)$$

where the EW and the non-CCB vacua have been identified to write  $m_t = Y_t < H_2 >_{EW}$ . The equalities on the right hand side of the equivalence eq.(43) signal that for this particular values of the soft squark masses, we are at the center of a critical regime where the CCB vacuum interferes with EW vacuum. This critical regime actually extends to a small range in  $m_{\tilde{t}_L}, m_{\tilde{t}_R}$  around this center, and is more generally characterized by the relation  $A_t^{inst} = A_{t,3}^c$ , meaning that no dangerous CCB vacuum, deeper than the EW vacuum, may develop unless the EW vacuum is unstable. In this region, there is also typically no room for a CCB vacuum to develop, not even a local one. This occurs already, e.g., at the center of the critical regime, where we have  $A_t^{inst} = A_t^{suf} = [A_t^{(0)}]$ . As will be illustrated in sec.5 [see Fig.4], this critical regime includes a small domain around this center where the typical hierarchy  $A_t^{(1)} \geq A_t^{(0)}$  is slightly violated, giving  $A_t^{suf} = A_t^{(0)}$ , and which is itself bordered by a domain where this hierarchy is respected, giving  $A_t^{suf} = A_t^{(1)}$ . We come now more precisely to the relation between the critical CCB bound  $A_{t,3}^c$ , eq.(27),

and the requirement of avoiding a tachyonic lightest stop. Obviously, this relation is crucial in the interference regime  $m_{\tilde{t}_L} m_{\tilde{t}_R} \sim m_t^2$ , corresponding to the case ii), where we have  $A_t^{inst} = A_{t,3}^c$ . With the help of the extremal equations, it is a straightforward exercise to show that for  $A_t \rightarrow A_t^{inst} [= A_{t,3}^c]$ , the VEVs of the CCB extremum verify  $(\langle H_2 \rangle, \langle \tilde{t}_{L,R} \rangle) \rightarrow (\langle H_2 \rangle_{\overline{EW}}, 0)$ , with furthermore:

$$\langle f \rangle \rightarrow \sqrt{\frac{12(m_{\tilde{t}_L}^2 + Y_t^2 \langle H_2 \rangle_{\overline{EW}}^2) + (g_1^2 - 3g_2^2) \langle H_2 \rangle_{\overline{EW}}^2}{12(m_{\tilde{t}_R}^2 + Y_t^2 \langle H_2 \rangle_{\overline{EW}}^2) - 4g_1^2 \langle H_2 \rangle_{\overline{EW}}^2}} \quad (44)$$

This particular direction is, in fact, connected to the direction of the lightest stop eigenstate. Let us denote  $(\bar{t}_1, \bar{t}_2)$  the stop-like eigenstates of the  $2 \times 2$  lower matrix in  $\mathcal{M}^2|_{\overline{EW}}$ , eq.(38), and  $\bar{\theta}$  the mixing angle of the rotation matrix  $\mathcal{R}$  relating these eigenstates to the VEVs  $(\langle \tilde{t}_L \rangle, \langle \tilde{t}_R \rangle)$ :

$$\begin{pmatrix} \bar{t}_1 \\ \bar{t}_2 \end{pmatrix} = \mathcal{R} \begin{pmatrix} \langle \tilde{t}_L \rangle \\ \langle \tilde{t}_R \rangle \end{pmatrix} \quad \text{with} \quad \mathcal{R} \equiv \begin{pmatrix} \cos \bar{\theta} & \sin \bar{\theta} \\ -\sin \bar{\theta} & \cos \bar{\theta} \end{pmatrix} \quad (45)$$

As noted before, if we assume that  $\tan \beta$  is large enough and  $|\mu| \ll |A_t| \tan \beta$ , we may safely identify this matrix with the physical squared stop matrix, and  $(\bar{t}_1, \bar{t}_2, \bar{\theta})$  with the stop eigenstates and mixing angle  $(\tilde{t}_1, \tilde{t}_2, \tilde{\theta})$  [1].

By definition, for  $A_t \rightarrow A_t^{inst}$ , the matrix  $\mathcal{M}^2|_{\overline{EW}}$ , eq.(38), has one zero eigenvalue and the wall separating the CCB extremum and the non-CCB extremum, lowers and eventually disappears in the direction of the corresponding eigenstate  $\bar{t}_1$ . In the basis  $(\tilde{t}_L, \tilde{t}_R)$ , the components of this eigenstate read  $\bar{t}_1 = (\bar{t}_1^L = \cos \bar{\theta}, \bar{t}_1^R = \sin \bar{\theta})$  and prove to verify

$$\tan \bar{\theta} \equiv \frac{\bar{t}_1^R}{\bar{t}_1^L} = \langle f \rangle \quad (46)$$

where  $\langle f \rangle$  is given by the limiting value in eq.(44). This shows on one hand that, in this critical regime, the stop mixing angle  $\bar{\theta}$  is related in a simple way to the deviation of the CCB vacuum from the  $SU(3)_c$  D-flat direction and, on the other, that taking into account such a deviation of the CCB vacuum to evaluate the critical CCB bound  $A_{t,3}^c$ , eq.(27), is crucial to avoid a tachyonic lightest stop.

## 4 Radiative corrections

In this section, we discuss the renormalization scale at which the tree-level necessary and sufficient condition to avoid CCB,  $A_t \leq A_{t,3}^c$ , eq.(27), should be evaluated in order to incorporate leading one-loop corrections. As is well-known, on a general ground, the complete, all order effective potential  $V(\phi)$  is a renormalization group invariant. However, this property is not shared by the tree-level approximation  $V^{(0)}$  which typically depends strongly on the renormalization scale  $Q$  at which it is computed [6, 15]. A kind of renormalization group-improved version of the tree-level potential which would incorporate a

resummation of all leading logarithmic contributions would certainly be more reliable. However, one faces here the tricky problem of dealing with many mass scales <sup>5</sup>. A better approximation to  $V(\phi)$ , more stable with respect to the scale  $Q$ , is in fact given by the one-level effective potential ( $\overline{MS}$  scheme) [6, 15]

$$V^{(1)}(\phi) = V^{(0)}(\phi) + \sum_i \frac{(-1)^{2s_i}(2s_i + 1)}{64\pi^2} M_i^4(\phi) \left[ \text{Log} \frac{M_i^2(\phi)}{Q^2} - \frac{3}{2} \right] \quad (47)$$

where  $M_i^2(\phi)$  denotes the tree-level squared mass of the eigenstate labeled  $i$ , of spin  $s_i$ , in the scalar field direction  $\phi$ . The scale  $Q$  enters explicitly in the one-loop correction, but also implicitly in the running of the mass and coupling parameters.

Obviously, in the field direction  $(H_2, \tilde{t}_L, \tilde{t}_R)$  studied in this paper, such a one-loop correction will introduce very complicated field contributions which will modify the simple tree-level geometrical picture presented here. However, we may still have "locally" a good indication of the impact of these radiative corrections with the help of our tree-level investigation. As is also well-known, around some scale  $Q_0$  which depends on the field direction considered, the predictions obtained with the tree-level potential  $V^{(0)}$  and the one-loop level potential  $V^{(1)}$  approximately coincide [6, 15]. This numerical observation was in fact intensively used, in particular in the context of CCB studies [6, 7, 8, 9, 10], precisely in order to use the relative simplicity of the tree-level potential. This field-dependent scale  $Q_0$  is typically of the order of the most significant mass present in the field region investigated. This roughly means that we reduce the multi-scale problem to a one-scale one, the "most significant mass" meaning a kind of average of the field-dependent masses which provide the leading one-loop contributions in the direction of interest [6, 15].

At the EW vacuum, it has been shown that the appropriate renormalization scale  $Q_{SUSY}$  where the one-loop corrections to the tree-level potential  $V|_{EW}$ , eq.(23), can be safely neglected is an average of the typical SUSY masses [6, 15]. For instance, for large  $M_{SUSY} \sim m_{\tilde{t}_L} \sim m_{\tilde{t}_R} \gg m_t$ , the tree-level potential receives important radiative corrections coming from loops of top and stop fields. In this case,  $Q_{SUSY}$  is expected to be an average of the top and stop masses, giving  $Q_{SUSY} \sim M_{SUSY}$ , whereas for low  $M_{SUSY} \lesssim m_t$ , this scale is somewhat underestimated and should be raised to a more typical SUSY mass [6, 15]. In this light, we see that we may trust the results obtained with the tree-level potential  $V|_{EW}$ , eq.(23), in particular the EW VEVs  $(v_1, v_2)$  given by eqs.(24, 25) and the depth of the EW potential  $\langle V \rangle|_{EW}$ , eq.(26), provided all parameters entering this potential are evaluated at the appropriate scale  $Q \sim Q_{SUSY}$ .

What is now the appropriate scale  $Q_{CCB}$  where the results obtained with the tree-level potential  $V_3$ , eq.(1), incorporate leading one-loop corrections? At the CCB vacuum, such corrections are expected to be induced by loops involving masses in the scalar field direction  $(H_2, \tilde{t}_L, \tilde{t}_R)$ , in particular for  $m_{\tilde{t}_L} \sim m_{\tilde{t}_R} \gg m_t$  for which these contributions are enhanced. Accordingly, we estimate  $Q_{CCB}$  to be an certain average of these masses, more precisely  $Q_{CCB} \sim \sqrt{\frac{\langle Tr \mathcal{M}^2 \rangle|_{CCB}}{3}}$ , where:

$$\langle Tr \mathcal{M}^2 \rangle|_{CCB} = \frac{1}{2} \left\langle \frac{\partial^2 V_3}{\partial H_2^2} + \frac{\partial^2 V_3}{\partial \tilde{t}_L^2} + \frac{\partial^2 V_3}{\partial \tilde{t}_R^2} \right\rangle|_{CCB} \quad (48)$$

---

<sup>5</sup>Some attempts have been made in this direction, see [20]

$$\begin{aligned}
&= m_{\tilde{t}_L}^2 + m_{\tilde{t}_R}^2 + Y_t^2[2H_2^2 + \tilde{t}_L^2(f^2 + 1)] + A_t Y_t f \frac{\tilde{t}_L^2}{H_2} \\
&\quad + \frac{g_1^2}{36}[9H_2^2 + (44f^2 - 1)\tilde{t}_L^2] + \frac{g_2^2}{4}(H_2^2 + 3\tilde{t}_L^2) + \frac{2g_3^2}{3}\tilde{t}_L^2(1 + f^2) \quad (49)
\end{aligned}$$

All fields should be evaluated at the CCB vacuum. To derive the last expression, we have used the extremal equation  $\partial V_3/\partial H_2 = 0$  to replace the Higgs mass parameter  $m_2$ . The VEV  $\langle \tilde{t}_L \rangle$  may also be replaced with the help of the extremal equation eq.(5-6), giving a complicated expression for  $Q_{CCB}$  which depends only on the soft terms  $A_t, m_{\tilde{t}_L}, m_{\tilde{t}_R}$ , the gauge and Yukawa couplings and the CCB VEVs  $\langle H_2 \rangle, \langle f \rangle$ . For simplicity, let us take  $M_{SUSY} = m_{\tilde{t}_L} = m_{\tilde{t}_R}$ , which gives  $\langle f \rangle = 1$ . Taking furthermore  $Y_t, g_3 \sim 1$ , neglecting other gauge couplings and (over-)estimating the VEV  $\langle H_2 \rangle \sim A_t/2$  [see eq.(30)], we find

$$Q_{CCB}^2 \sim \frac{11A_t^2 - 20M_{SUSY}^2}{18} \quad (50)$$

This scale is meaningful only when a CCB vacuum develops, that is for  $A_t \geq A_t^{suf}$  [see eq.(34)]. For illustration, we estimate roughly this lower bound with  $A_t^{(0)}$ , eq.(9). Taking  $A_t \sim 2 M_{SUSY}$ , we obtain  $Q_{CCB} \sim 1.33 M_{SUSY}$ . Let us stress here that a refined evaluation of  $Q_{CCB}$ , with realistic values for the gauge couplings, the CCB VEV  $\langle H_2 \rangle$  and the optimal sufficient bound  $A_t^{suf}$ , would give in fact a value for  $Q_{CCB}$  closer to  $M_{SUSY}$ . This simple illustration however already provides a clear indication that  $Q_{CCB}$  is typically of order  $M_{SUSY}$ .

For  $M_{SUSY} \gg m_t$  and  $A_t \gtrsim A_t^{suf}$ , we conclude therefore that we have  $Q_{CCB} \sim Q_{SUSY}$ . Obviously, a similar conclusion is expected in the complementary regime  $M_{SUSY} \lesssim m_t$ : in this case, the CCB and the EW vacua prove to be close, implying a mass spectrum of the same order at each vacuum. We note also that this estimation of  $Q_{CCB}$  is in full agreement with the one obtained in ref.[6] in the extended plane  $(H_1, H_2, \tilde{t}_L, \tilde{t}_R)$ . In this article, the scale  $Q_{CCB}$  was estimated to be  $\sim \text{Max}[Q_{SUSY}, g_3 A_t/4Y_t, A_t/4]$ , which reduces for  $Y_t, g_3 \sim 1$  and  $A_t \gtrsim A_t^{suf} \gtrsim 2M_{SUSY}$  to  $Q_{CCB} \sim Q_{SUSY}$ .

Two important conclusions can be deduced from this result. On one hand, we see that the optimal sufficient bound  $A_t^{suf}$ , eq.(34), should be evaluated at  $Q_{CCB} \sim Q_{SUSY}$ , in order to minimize the one-radiative corrections to the tree-level potential  $V_3$ , eq.(1). More importantly, we see that, at this common scale  $Q_{CCB} \sim Q_{SUSY}$ , it is also meaningful to compare the tree-level depth of the potential at the EW vacuum, i.e.  $\langle V \rangle|_{EW}$ , eq.(26), and at the CCB vacuum, in order to determine the necessary and sufficient condition  $A_t \leq A_{t,3}^c$ , eq.(27), to avoid CCB in the plane  $(H_2, \tilde{t}_L, \tilde{t}_R)$ . This point is a mere consequence of the fact that the potential at a realistic EW vacuum is not very deep, as already noted in sec.3.3 [see eq.(35)], therefore giving  $A_{t,3}^c \gtrsim A_t^{suf}$ . To summarize, we expect our tree-level refined CCB bounds to be robust under inclusion of leading one-loop corrections to the potential, provided they are evaluated at  $Q \sim Q_{SUSY}$ . Accordingly, stability of the EW vacuum in the plane  $(H_2, \tilde{t}_L, \tilde{t}_R)$  should be tested in model-dependent scenarii [3, 4, 6] at this scale.

## 5 Practical guide to evaluate the CCB conditions

Let us now collect and summarize the main results we have found. As mentioned in sec.2.3, the evaluation of the critical bound  $A_{t,3}^c$ , eq.(27), above which there is CCB in the plane  $(H_2, \tilde{t}_L, \tilde{t}_R)$  requires the precise determination of the CCB VEVs and comparison of the potential  $V_3$ , eq.(1), at the CCB vacuum with the value of the potential at the EW vacuum  $\langle V \rangle|_{EW}$ , eq.(26). This comparison is meaningful and incorporates leading one-loop corrections, provided all parameters are evaluated at the appropriate renormalization scale  $Q \sim Q_{SUSY}$ , where  $Q_{SUSY}$  is an average of the typical SUSY masses at a realistic EW vacuum. This assumption will be implicitly made in the following. Accordingly, the main practical steps to evaluate  $A_{t,3}^c$  are:

- **Evaluation of the depth of the EW potential:** take a realistic set of values for  $g_1, g_2, g_3$  consistent with experimental data; choose in addition values for  $\tan \beta$  and the pseudo-scalar mass  $m_{A^0}^2 = m_1^2 + m_2^2$ . The top mass  $m_t = Y_t v \sin \beta$ , with  $v = 174 \text{ GeV}$ , determines the value of the top Yukawa coupling  $Y_t$ . Finally, the extremal equations in the EW direction eqs.(24,25) determine the Higgs mass parameters  $m_1, m_2, m_3$  and the depth of the potential at the EW vacuum  $\langle V \rangle|_{EW}$ , eq.(26).

- **Evaluation of the CCB optimal sufficient bound:** choose a set of values for the soft mass parameters  $m_{\tilde{t}_L}, m_{\tilde{t}_R}$  and evaluate the optimal sufficient bound  $A_t^{suf} = \text{Max}[A_t^{(0)}, A_t^{(1)}]$ , eq.(34). This requires the comparison of the quantities  $A_t^{(0)}$  given by eq.(9), and  $A_t^{(1)}$  given by the largest solution in  $A_t$  of the equation  $\mathcal{C}_3 = 0$ , eq.(33). To evaluate  $A_t^{(1)}$ , the parameter  $f$  of the departure of the CCB vacuum from the  $SU(3)_C$  D-flat direction should be taken at the excellent approximated value  $f_3^{(0)}$ , eq.(31) [see sec.3.2]. The value obtained  $A_t^{suf}$  is the optimal sufficient bound to avoid CCB. This means that for  $A_t = A_t^{suf}$  a CCB local vacuum, not necessarily global, begins to develop in the plane  $(H_2, \tilde{t}_L, \tilde{t}_R)$ , and soon becomes global as  $A_t$  increases. This bound therefore considerably simplifies the determination of the necessary and sufficient bound  $A_{t,3}^c$  to avoid CCB in this plane.

For  $1 \leq \tan \beta \leq \sqrt{1 + 2m_{A^0}^2/m_{Z^0}^2}$ , or equivalently  $m_2^2 \geq 0$ , we always have  $A_t^{suf} = A_t^{(1)}$  [see sec.3.4]. In the complementary regime, we have  $m_2^2 \leq 0$ , and an additional non-CCB vacuum develops in the plane  $(H_2, \tilde{t}_L, \tilde{t}_R)$ . For large enough  $\tan \beta$ , it essentially coincides with the EW vacuum which is located in the vicinity of this plane [see sec.3.4]. As a result, a new computable instability bound  $A_t^{inst}$ , eqs.(39,40), appears. This bound merely reflects the physical requirement of avoiding a non-tachyonic lightest stop, for large  $\tan \beta$ . Besides, an inversion of the typical hierarchy between the sufficient bounds  $A_t^{(0)} \leq A_t^{(1)}$  may occur, implying  $A_t^{suf} = A_t^{(0)}$ . This inversion however takes place only in the critical region  $m_{\tilde{t}_L} m_{\tilde{t}_R} \sim m_t$  where the CCB vacuum interferes with the non-CCB vacuum aforementioned. In this interference regime, the instability bound  $A_t^{inst}$  is quite restrictive and the relation  $A_t^{suf} \leq A_{t,3}^c \leq A_t^{inst}$ , eq.(41), is saturated on both sides, meaning that no dangerous CCB vacuum may develop unless the EW vacuum is unstable.

Whatever the value of  $\tan \beta$ , for large enough soft masses  $m_{\tilde{t}_L}, m_{\tilde{t}_R} \gtrsim 300 \text{ GeV}$ , a good

approximation to the bound  $A_t^{suf}$  is given by  $A_t^{ap}$ , eq.(36) [see sec.3.3].

Let us remark that the parameters involved in these first two steps, basically  $(m_{A^0}, \tan \beta, m_{\tilde{t}_L}, m_{\tilde{t}_R})$ , are typical of phenomenological model-independent Higgs studies, the benchmark scenario  $M_{SUSY} = m_{\tilde{t}_L} = m_{\tilde{t}_R}$  being often considered [13]. Once such a set of values is chosen, CCB considerations induce an additional constraint on the allowed values for the trilinear soft term  $A_t$ .

• **Evaluation of the CCB critical bound  $A_{t,3}^c$ :** the determination of the CCB VEVs and comparison of the depth of the CCB potential  $V_3$ , eq.(1), and  $\langle V \rangle|_{EW}$ , eq.(26), is needed [see sec.2.3]. This step requires a numerical scan of the region  $A_t \geq A_t^{suf}$ , which is not time consuming, because typically the critical bound  $A_{t,3}^c$  proves to be just slightly above the optimal sufficient bound  $A_t^{suf}$  previously determined. The computation of the CCB VEVs may be achieved with the help of the algorithm presented in sec.3.1. The main steps are the following:

- Solve the extremal equation eq.(14) in  $H_2$  with the initial input  $f = f_3^{(0)}$  given by eq.(31). For  $A_t \geq A_t^{suf}$ , this cubic equation in  $H_2$  has necessarily three real positive roots [see sec.3.3]. The intermediate solution, denoted  $H_2^{(0)}$ , which can be given an explicit analytical expression, always proves to be very close to the CCB VEV  $\langle H_2 \rangle$  (the discrepancy is less than 1%).

- Solve the extremal equation eq.(19) in  $f$  with  $H_2 = H_2^{(0)}$ . This equation has only one consistent (i.e. real and positive, see sec.2.2) solution  $f^{(1)}$ , which is even closer to the CCB VEV  $\langle f \rangle$  than  $f_3^{(0)}$ .

- The algorithm may be iterated in the same way without ambiguity. The set of values  $(H_2^{(n)}, f^{(n)})_{n \geq 0}$  proves to converge very fast towards  $(\langle H_2 \rangle, \langle f \rangle)$ .

Once the CCB VEVs  $\langle H_2 \rangle, \langle f \rangle$  are computed,  $\langle \tilde{t}_L \rangle$  is obtained by eq.(5) and we have  $\langle \tilde{t}_R \rangle = \langle f \rangle \langle \tilde{t}_L \rangle$ , which completes the determination of the location of the CCB vacuum. The final step is the comparison of the potential  $V_3$ , eq.(1), at this dangerous vacuum with  $\langle V \rangle|_{EW}$ . A scan for  $A_t \geq A_t^{suf}$  then provides the critical bound  $A_{t,3}^c$ .

For completeness, we have summarized the full algorithm to compute the critical bound  $A_{t,3}^c$ . It is however important to stress that, in practice, this evaluation is considerably simpler and more rapid. The values  $(H_2^{(0)}, f_3^{(0)})$  obtained with the first iteration of our algorithm already provide excellent analytic approximations of  $(\langle H_2 \rangle, \langle f \rangle)$ . Further iterations will result in unimportant effects. In particular, the impact on the critical CCB bound  $A_{t,3}^c$  is extremely tiny,  $\sim O(1 \text{ GeV})$ . Thus, to an excellent accuracy, explicit analytic expressions for all the VEVs of the CCB vacuum and of the potential  $V_3$ , eq.(1), at this vacuum can be given, and the determination of the critical CCB bound  $A_{t,3}^c$  essentially reduces to the comparison of the CCB potential  $V_3$ , eq.(1), at the CCB vacuum with the EW potential  $\langle V \rangle|_{EW}$ , eq.(26).

## 6 Numerical illustration of the CCB bounds

We turn now to the numerical illustration of the various CCB bounds obtained in the plane  $(H_2, \tilde{t}_L, \tilde{t}_R)$ , first for low  $\tan\beta$  [we take  $\tan\beta = 3$ ], and then for large  $\tan\beta$  [we consider the limiting case  $\tan\beta = +\infty$ ], where the additional negative contribution of the Higgs mass parameter  $m_2^2$  induces new features of the potential, as shown in sec.3.4. In order to incorporate one-loop leading corrections, the CCB bounds are implicitly supposed to be evaluated at the SUSY scale  $Q \sim Q_{SUSY}$ .

### • The low $\tan\beta$ regime

In Figures 2-3, the behaviour of the CCB bounds on  $A_t$ , i.e. the critical bound  $A_{t,3}^c$ , eq.(27), the optimal sufficient bound  $A_t^{suf}$ , eq.(9), which is always equal  $A_t^{(1)}$  in this regime, its approximation  $A_t^{ap}$ , eq.(36), and finally the traditional bound in the D-flat direction  $A_{t,3}^D$ , eq.(2), is illustrated as a function of the soft squark masses  $m_{\tilde{t}_L}, m_{\tilde{t}_R}$ . The set of values chosen is consistent with a correct tree-level EW symmetry breaking with  $\tan\beta = 3, m_{A^0} = 520 \text{ GeV}$  and a top quark mass  $m_t = 175 \text{ GeV}$ . As can be seen, in both illustrations, the hierarchy  $A_{t,3}^c \geq A_t^{suf} = A_t^{(1)}$ , eq.(35), is verified, as expected.

In Figure 2, the various CCB bounds are plotted as a function of the ratio  $r_1 = m_{\tilde{t}_L}/m_{\tilde{t}_R}$ , taking  $m_{\tilde{t}_R} = 200 \text{ GeV}$ . Therefore, except for  $r_1 = 1$ , the CCB vacuum always deviates from the  $SU(3)_c$  D-flat direction. Comparing the critical bound  $A_{t,3}^c$  and  $A_t^{(1)}$ , we see that they follow each other closely for all values of  $r_1$ , with  $A_{t,3}^c \sim 1.04 - 1.10 A_t^{(1)}$ , the lowest values being reached for large  $r_1$  and the largest for  $r_1 \sim 0$ . For  $1 \lesssim r_1 \leq 5$ , the sufficient bound  $A_t^{(1)}$  is approximately linear in  $r_1$  and the accuracy of the approximation  $A_t^{ap}$  is rather good, better than 5%. Although this linear behaviour breaks down for low  $r_1 \lesssim 1$ ,  $A_t^{ap}$  still provides a good thumbrule to evaluate  $A_t^{(1)}$  (within 5 – 8%). Note that we can have either  $A_t^{(1)} \geq A_t^{ap}$  or  $A_t^{(1)} \leq A_t^{ap}$ , showing that  $A_t^{ap}$  is just an approximation and should be handled with care.

For  $r_1 \sim 1$ , we have  $A_{t,3}^D \sim A_t^{(1)} \sim A_{t,3}^c$ . In this regime, the soft squark masses are of the same order, implying that the CCB vacuum is nearly aligned in the  $SU(3)_c$  D-flat direction, as noted in sec.3.4. The CCB vacuum is also located in the vicinity of the  $SU(2)_L \times U(1)_Y$  D-flat direction, because the common value of the soft squark masses  $m_{\tilde{t}_L} \sim m_{\tilde{t}_R} \sim 200 \text{ GeV}$  is not so large compared to the Higgs mass parameter  $m_2 = 118 \text{ GeV}$ , so that the relation eq.(3) is approximately verified [see sec.2.1, eq.(3)]. For large  $r_1 \sim 5$  and  $A_t \sim A_{t,3}^c$ , the CCB vacuum is located far away from the  $SU(3)_c$  D-flat direction (as well as the  $SU(2)_L \times U(1)_Y$  D-flat direction). This large departure clearly appears by comparing the traditional CCB bound in the D-flat direction,  $A_{t,3}^D \sim 1778 \text{ GeV}$ , and the critical bound  $A_{t,3}^c \sim 1383.5 \text{ GeV}$ . The latter is about 30% below the traditional bound  $A_{t,3}^D$ ! This is a typical feature of this D-flat direction condition: for large soft squark masses, it is far from being optimal and not very indicative of the critical bound  $A_{t,3}^c$ . A better estimate is given by the optimal sufficient bound  $A_t^{(1)}$  or even its approximation  $A_t^{ap}$ .

Finally, we note that if we had taken  $r_{-1} = m_{\tilde{t}_R}/m_{\tilde{t}_L}$  and  $m_{\tilde{t}_R} = 200 \text{ GeV}$ , the curves



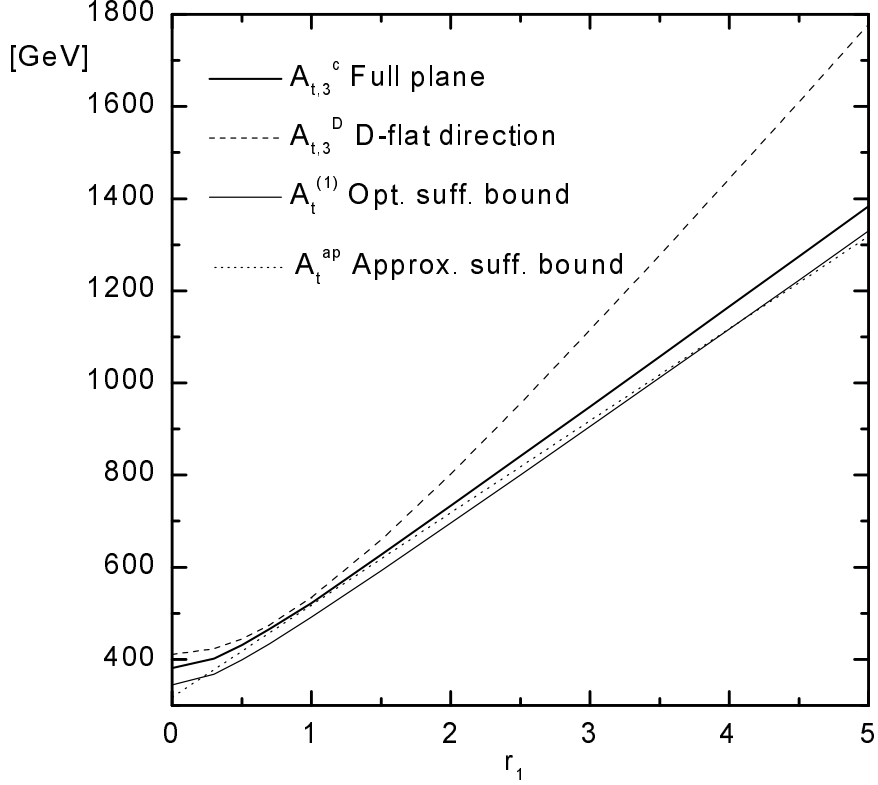


Figure 2: CCB bounds versus  $r_1 = m_{\tilde{t}_L}/m_{\tilde{t}_R}$ . We take  $m_{\tilde{t}_R} = 200$  GeV,  $m_1 = 400$  GeV,  $m_3 = 228$  GeV and  $m_2, Y_t, g_1, g_2, g_3$  as in Fig.1. This gives  $m_t = 175$  GeV.

obtained would overlap the ones presented here. This is obviously an exact result for  $A_{t,3}^D, A_t^{ap}$  [see eqs.(2,36)], but it proves also to occur to a very good approximation for  $A_{t,3}^c, A_t^{(1)}$ .

In Figure 3, the various CCB bounds are now plotted as a function of  $M_{SUSY} = m_{\tilde{t}_L} = m_{\tilde{t}_R}$ , with the same set of values as in Fig.2 for the other parameters. The CCB vacuum is now automatically aligned in the  $SU(3)_c$  D-flat direction, but not the in  $SU(2)_L \times U(1)_Y$  D-flat one, except for  $M_{SUSY} = m_2 = 118$  GeV, see eq.(3).

In this illustration, we recover the same qualitative behaviour of the CCB bounds as in Fig.2. Comparing this illustration with the previous one for an equal value of  $M_{SUSY}^2 = (m_{\tilde{t}_L}^2 + m_{\tilde{t}_R}^2)/2$ , we furthermore observe that the difference  $|A_{t,3}^D - A_{t,3}^c|$  is smaller in Fig.3 than in Fig.2, precisely because of this alignment in the  $SU(3)_c$  D-flat direction. In Fig.2, for instance, for  $M_{SUSY}^2 = (720 \text{ GeV})^2$  with  $r_1 = 5$ , the critical bound  $A_{t,3}^c$  is about 22% below the traditional bound  $A_{t,3}^D$ , whereas for an equal value of  $M_{SUSY} = 720$  GeV in Fig.3, which gives the same value for  $A_{t,3}^D$ , the critical bound  $A_{t,3}^c$  is now just about 10% below  $A_{t,3}^D$ . This illustrates the fact that any departure of the CCB vacuum from the  $SU(3)_c$  D-flat direction or, equivalently, any splitting between the soft squark masses, tends to lower substantially the critical bound  $A_{t,3}^c$  below which there is no CCB danger.

### • The large $\tan \beta$ regime

Figure 4 is devoted to the large  $\tan \beta$  regime. We take  $M_{SUSY} \equiv m_{\tilde{t}_L} = m_{\tilde{t}_R}$ , with

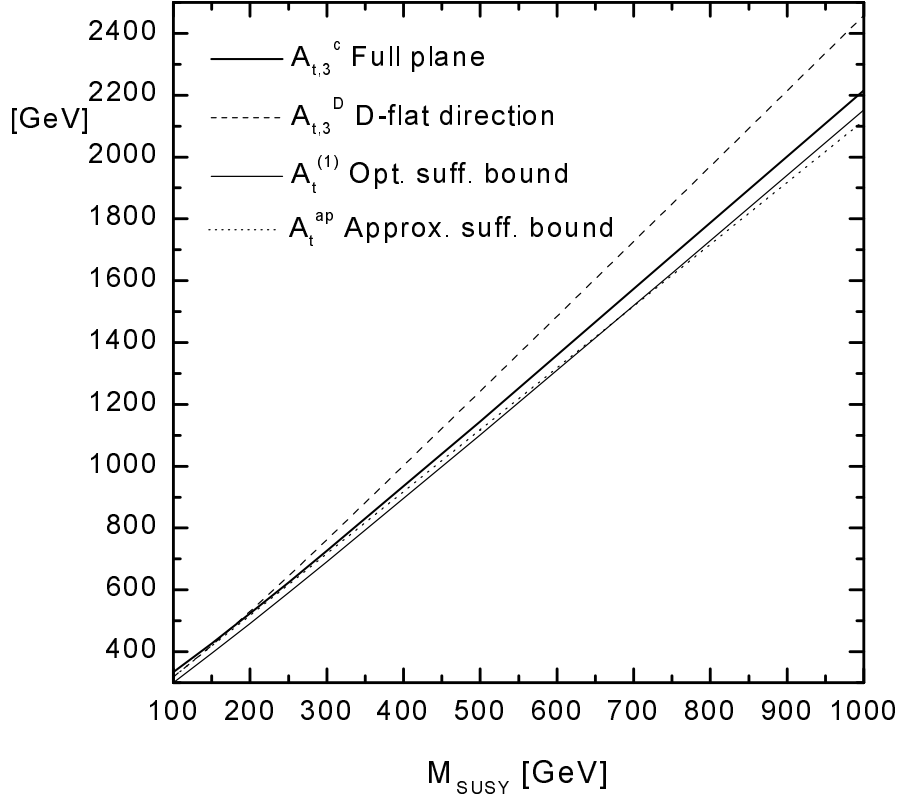


Figure 3: CCB bounds versus  $M_{SUSY} = m_{\tilde{t}_L} = m_{\tilde{t}_R}$ . Same set of values as in Fig.1-2 for the other parameters.

$\tan \beta = +\infty$ . This benchmark scenario is often considered in Higgs phenomenology [13, 14] and this illustration is presented to set the stage for the next section where the impact of the CCB conditions on the stop mass spectrum and on the one-loop upper bound on the lightest Higgs mass,  $m_h$ , will be considered. As will be shown in a forthcoming article [11], this extreme  $\tan \beta$  case also proves to be numerically representative of the large  $\tan \beta$  regime, i.e.  $\tan \beta \gtrsim 15$ , with furthermore  $|\mu| \lesssim \text{Min}[m_{A^0}, M_{SUSY}]$ .

In this benchmark scenario, the CCB vacuum is automatically aligned in the  $SU(3)_c$  D-flat direction. Obviously, any discrepancy between the soft mass terms  $m_{\tilde{t}_L}, m_{\tilde{t}_R}$  would induce a deviation from this direction and, on the other hand, a numerical modification of the CCB bounds illustrated here, but the qualitative behaviour of the CCB bounds would remain the same.

For  $\tan \beta = +\infty$ , the EW vacuum is trapped in the plane  $(H_2, \tilde{t}_L, \tilde{t}_R)$  and the depth of the EW potential is determined to be  $\langle V \rangle_{EW} = -m_{Z^0}^4 / 2(g_1^2 + g_2^2)$  [see sec.3.4]. Figure 4 illustrates how this geometrical feature of the potential affects the various CCB bounds, including the sufficient bound  $A_t^{(0)}$ , eq.(9), and the instability bound  $A_t^{inst}$ , eqs.(39,40).

For all  $M_{SUSY}$ , the hierarchy  $A_t^{suf} \equiv \text{Max}[A_t^{(0)}, A_t^{(1)}] \leq A_{t,3}^c \leq A_t^{inst}$  is respected, even in the critical region  $M_{SUSY} \sim m_t$ . This hierarchy merely reflects the fact that, on one hand, no CCB vacuum may develop for  $A_t \leq A_t^{suf}$ , implying  $A_{t,3}^c \geq A_t^{suf}$ . On the other, if  $A_t \geq A_t^{inst}$ , the EW vacuum would be automatically unstable and would bend down in the direction of a deeper CCB vacuum, which implies necessarily  $A_t^{inst} \geq A_{t,3}^c, A_t^{suf}$ .

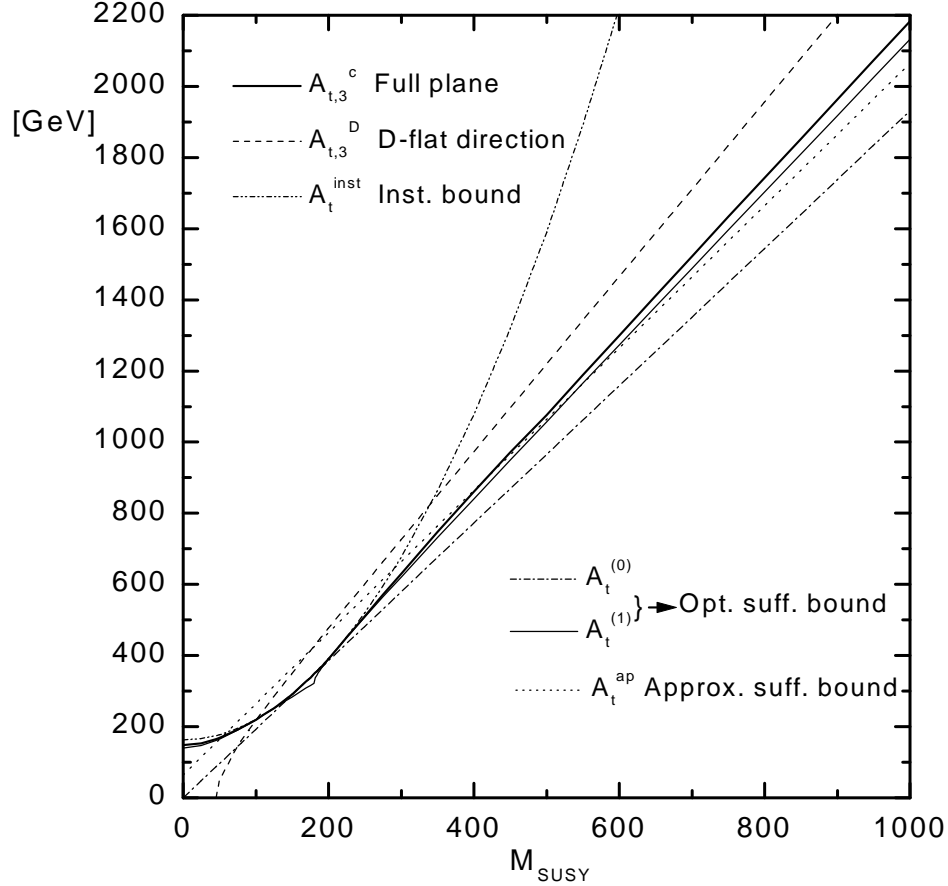


Figure 4: CCB bounds versus  $M_{SUSY} \equiv m_{\tilde{t}_R} = m_{\tilde{t}_L}$ , for  $\tan\beta = +\infty$ . The optimal sufficient bound is  $A_t^{suf} \equiv \text{Max}[A_t^{(0)}, A_t^{(1)}]$ . We take  $m_2^2 = -m_{Z^0}^2/2$  [see eq.(24)] and  $m_t = 175 \text{ GeV}$  which implies  $Y_t = 1$ .

For all  $M_{SUSY}$ , the critical bound  $A_{t,3}^c$  is just above the optimal sufficient bound  $A_t^{suf}$ . For instance, for  $M_{SUSY} \geq 210 \text{ GeV}$ , we have  $A_t^{suf} \leq A_{t,3}^c \lesssim 1.02 A_t^{suf}$ , with  $A_t^{suf} = A_t^{(1)}$ . This shows once again how an accurate approximation  $A_t^{suf}$  can be for the critical CCB bound  $A_{t,3}^c$ . We note also that  $A_t^{ap}$  provides a good estimate of  $A_t^{suf}$ , at least for  $M_{SUSY} \geq 300 \text{ GeV}$ .

The traditional bound  $A_{t,3}^D$  in the D-flat direction exists only for  $M_{SUSY} \gtrsim 45.56 \text{ GeV}$ , and above this value it increases fast. Let us remark that for  $M_{SUSY} \lesssim 100 \text{ GeV}$ ,  $A_{t,3}^D$  is not a necessary upper bound on  $A_t$  to avoid CCB, because for  $A_t \in [A_{t,3}^D, A_{t,3}^c]$ , the CCB vacuum is not deeper than the EW vacuum and is therefore not dangerous. The traditional bound  $A_{t,3}^D$  provides a necessary condition to avoid CCB only for  $M_{SUSY} \gtrsim 100 \text{ GeV}$ , but in this case it is far from being sufficient. Typically much larger than the critical CCB bound  $A_{t,3}^c$ , it should also be handled with care. For instance, for  $M_{SUSY} \sim 300 \text{ GeV}$ , it allows for some values of  $A_t$  above the instability bound  $A_t^{inst}$ , implying a tachyonic lightest stop mass!

For  $110 \text{ GeV} \lesssim M_{SUSY} \lesssim 210 \text{ GeV}$ , the various CCB bounds  $A_t^{(0)}, A_t^{(1)}, A_{t,3}^c, A_t^{inst}$  cluster. The potential enters in the critical regime where the CCB vacuum interfere with the EW

vacuum. In this regime, the critical CCB bound  $A_{t,3}^c$  coincides with the instability bound  $A_t^{inst}$ , implying that a dangerous CCB vacuum may develop only if the lightest physical stop gets tachyonic. Included in this small region of the parameter space, more precisely for  $140 \text{ GeV} \lesssim M_{SUSY} \lesssim 192 \text{ GeV}$ , the typical hierarchy  $A_t^{(1)} \geq A_t^{(0)}$  is violated and we have therefore  $A_t^{suf} = A_t^{(0)}$ . We note however that the maximal discrepancy between  $A_t^{(0)}$  and  $A_t^{(1)}$  is quite small, less than  $5 \text{ GeV}$ .

Finally, we observe that for  $M_{SUSY} \gtrsim 300 \text{ GeV}$ , the critical CCB bound  $A_{t,3}^c$  is much lower than the instability bound  $A_t^{inst}$ . This result has an important physical consequence in the limiting case  $\tan \beta = +\infty$  considered here, for which the stop mixing parameter  $\tilde{A}_t$  coincides with the trilinear soft term  $A_t$ . It implies that the CCB critical bound  $A_{t,3}^c$  provides stringent restrictions on the mass spectrum of the stop quark fields. This important point is addressed in the next section.

## 7 The stop CCB maximal mixing

We investigate in this section some physical implications of the critical CCB bound on the stop mass spectrum and the one-loop upper bound on the lightest Higgs mass. We consider the benchmark scenario  $M_{SUSY} = m_{\tilde{t}_L}^2 = m_{\tilde{t}_R}^2$ , with  $\tan \beta = +\infty$  [13, 14]. As noted in the last section, this extreme  $\tan \beta$  regime is also quite representative numerically of the large  $\tan \beta$  regime with small  $\mu$ , i.e.  $\tan \beta \gtrsim 15$  and  $|\mu| \lesssim \text{Min}[m_{A^0}, M_{SUSY}]$  [11]. To be optimal, the extension to the low  $\tan \beta$  regime, valid for all values of  $\mu$ , requires an investigation of the extended plane  $(H_1, H_2, \tilde{t}_L, \tilde{t}_R)$ . This case will be presented in a separate article [11].

In the benchmark scenario considered here, the stop mixing parameter  $\tilde{A}_t = A_t + \mu / \tan \beta$  equals the trilinear soft term  $A_t$  and the squared stop mass matrix is given by the lower  $2 \times 2$  matrix of  $\mathcal{M}^2|_{\overline{EW}}$ , eq.(38), taking  $H_2 = v_2$ . Accordingly, the squared masses for the stop eigenstates read [1]:

$$m_{\tilde{t}_1, \tilde{t}_2}^2 = M_{SUSY}^2 + m_t^2 - \frac{1}{4}m_{Z^0}^2 \mp \frac{1}{2}\sqrt{4m_t^2 A_t^2 + \frac{(8m_{W^\pm}^2 - 5m_{Z^0}^2)^2}{6}} \quad (51)$$

These masses depend only on two free parameters,  $A_t$  and the unified soft squark mass  $M_{SUSY}$ . However, taking into account the CCB condition, a non-trivial correlation appears between these two parameters. To avoid CCB in the plane  $(H_2, \tilde{t}_L, \tilde{t}_R)$ , it is necessary and sufficient that  $A_t \leq A_{t,3}^c$ , eq.(27), where the dependence in  $M_{SUSY}$  of the critical bound  $A_{t,3}^c$  is plotted in Fig.4. In the following, all parameters are supposed to be evaluated at the appropriate renormalization scale  $Q \sim Q_{SUSY}$ , in order to incorporate one-loop leading corrections to this CCB bound.

In Figure 5, we compare the critical bound  $A_{t,3}^c$  to the so-called Higgs maximal mixing  $\tilde{A}_t^{max}$  commonly considered in Higgs phenomenology [13, 14]:

$$\tilde{A}_t^{max} = A_t^{max} = \sqrt{6}m_{\tilde{t}} \quad \text{with} \quad m_{\tilde{t}}^2 = M_{SUSY}^2 + m_t^2 \quad (52)$$

As is well-known, the lightest Higgs mass,  $m_h$ , receives a large one-loop correction arising

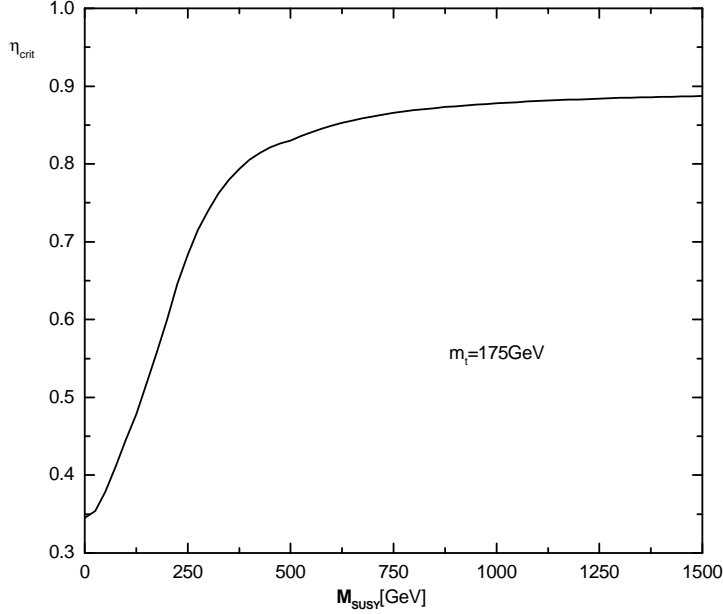


Figure 5: Critical CCB parameter  $\eta_{crit} \equiv A_{t,3}^c/A_t^{mix}$ , versus  $M_{SUSY}$  for large  $\tan\beta$ . Same set of parameters as in Fig.4.

from top and stop loops, proportional to  $m_t^4$  and which grows logarithmically with  $M_{SUSY}$ . This correction is essential to overcome the tree-level upper bound  $m_h \leq m_{Z^0}$  and is maximized for the Higgs maximal mixing, eq.(52) [13, 14]. We stress however that there is no physical reason to exclude stop mixing larger than this one, provided the masses obtained for the lightest stop and CP-even Higgs are not ruled out by experimental data. The prominent fact in Fig.5 is that  $\eta_{crit} \equiv A_{t,3}^c/A_t^{max}$  is well below unity. We have  $0.35 \leq \eta_{crit} \leq \frac{8}{9} \sim 0.89$  for  $M_{SUSY} \leq 1500$  GeV, showing that the CCB critical bound is at least 10% below the Higgs maximal mixing, eq.52). *Thus, the Higgs maximal mixing is always ruled out by CCB considerations!* Moreover, it can be shown that this striking result holds not only for large  $\tan\beta$ , but is also typically verified for low  $\tan\beta$  [11]. Actually, the lower  $\tan\beta$  is and the more CCB conditions will tend to rule out such a large stop mixing.

In the light of this new result, we introduce a new quantity, the "CCB maximal mixing", defined to be the largest stop mixing  $\tilde{A}_t$  allowed by CCB considerations. Obviously, in the case considered here, the CCB maximal mixing coincides with the critical value  $A_{t,3}^c$ , plotted in Fig.4. Such a maximal mixing has a clear physical meaning, which implies in particular that the lightest Higgs mass,  $m_h$ , cannot reach its maximal value [at one-loop level, for the Higgs maximal mixing, eq.(52)], unless the EW vacuum is unstable.

In Figure 6, we illustrate the bounds on the stop masses induced by the CCB maximal mixing as a function of  $M_{SUSY}$ , and compare them to the Higgs maximal mixing and also to the no mixing ( $A_t = 0$ ) cases. The lower curves correspond to the minimal values allowed for the mass of the lightest stop  $\tilde{t}_1$  and the upper to the maximal values allowed for the mass of the heaviest stop  $\tilde{t}_2$ .

As expected, the bounds on the stop masses induced by the CCB maximal mixing are more restrictive than for the Higgs maximal mixing. All stop mass values compatible

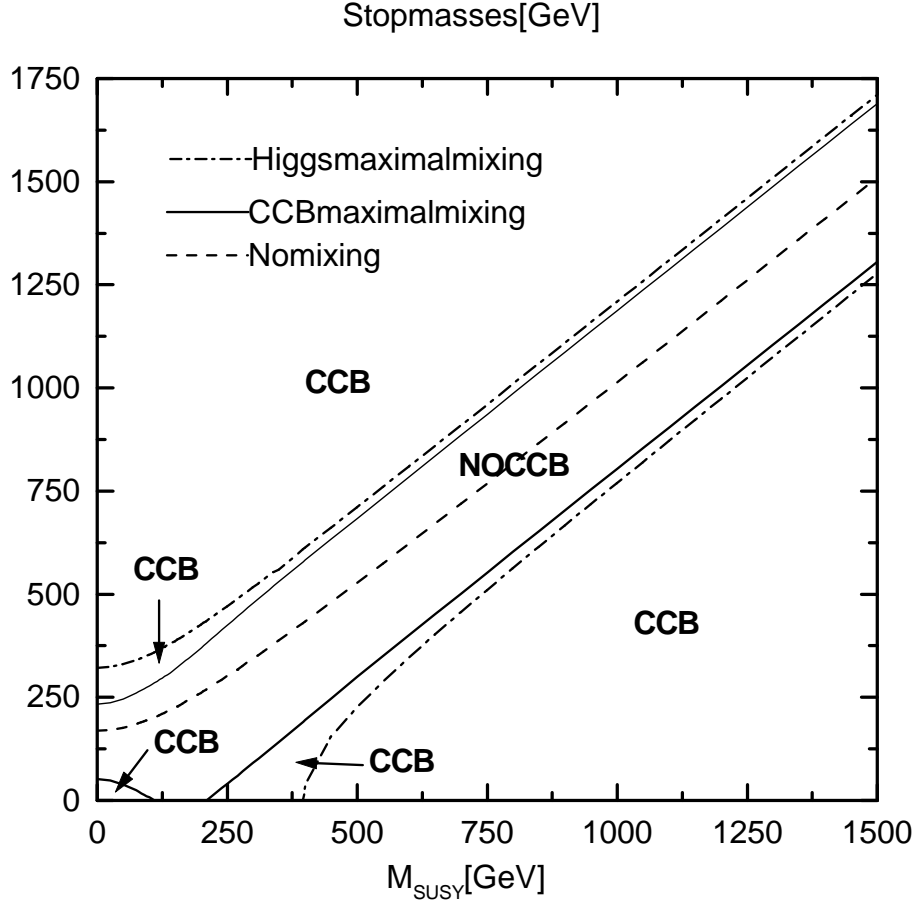


Figure 6: Exclusion domain for the stop masses versus  $M_{SUSY}$ , for  $\tan\beta = +\infty$ . The higher curves [above the no mixing curve] provide upper bounds on the mass of the heaviest stop  $\tilde{t}_2$ , and the lower [below the no mixing curve] lower bounds on the mass of the lightest stop  $\tilde{t}_1$ . Same set of parameters as in Fig.4.

with a Higgs maximal mixing are always located in the dangerous CCB region. For  $M_{SUSY} \lesssim 425 \text{ GeV}$ , the Higgs maximal mixing is already ruled out, either because it gives a tachyonic lightest stop [for  $M_{SUSY} \lesssim 400 \text{ GeV}$ ], or because the lightest stop is too light [we take conservatively  $m_{\tilde{t}_1} \gtrsim 100 \text{ GeV}$ ] and should have been already found experimentally [21]. In this region of small  $M_{SUSY}$ , the CCB maximal mixing enables us to avoid such a tachyonic lightest stop mass. For  $M_{SUSY} \lesssim 110 \text{ GeV}$ , the lower bound on the lightest stop mass slowly decreases with  $M_{SUSY}$  and becomes exactly zero for  $110 \text{ GeV} \lesssim M_{SUSY} \lesssim 210 \text{ GeV}$ . In this critical region, the CCB vacuum interferes with the EW vacuum and cannot be deeper than the latter, unless the lightest stop mass becomes tachyonic.

For  $M_{SUSY} \lesssim 310 \text{ GeV}$ , even the CCB maximal mixing is excluded by the conservative experimental bound  $m_{\tilde{t}_1} \gtrsim 100 \text{ GeV}$ . Therefore, in this region of low  $M_{SUSY}$ , the EW vacuum is necessarily the deepest one and cannot be metastable. This example illustrates how experimental limits on the lightest stop combined with a precise determination of the CCB condition may secure the EW vacuum in a large part of the parameter space, so that metastability considerations become completely irrelevant. In addition, we have also in this region the upper bound  $m_{\tilde{t}_2} \lesssim 490 \text{ GeV}$ .

For  $M_{SUSY} \gtrsim 310 \text{ GeV}$ , the bounds on the stop spectrum increase with  $M_{SUSY}$ . At  $M_{SUSY} = 500 \text{ GeV}$ , the discrepancies between the CCB maximal mixing and the Higgs maximal mixing cases are quite large for the lightest stop,  $\Delta m_{\tilde{t}_1} \sim 75 \text{ GeV}$ , and smaller but still important for the heaviest stop  $\Delta m_{\tilde{t}_2} \sim 30 \text{ GeV}$ . They tend to decrease slowly with  $M_{SUSY}$  and we have, e.g.,  $\Delta m_{\tilde{t}_1} \sim 30 \text{ GeV}$  and  $\Delta m_{\tilde{t}_2} \sim 20 \text{ GeV}$ , for  $M_{SUSY} = 1500 \text{ GeV}$ .

The linear behaviour of the CCB bounds on the stop masses for large  $M_{SUSY}$  is a direct consequence of the asymptotic behaviour of the critical parameter  $\eta_{crit} \lesssim 8/9 \sim 0.89$  [see Fig.5]. For  $M_{SUSY} \gtrsim 500 \text{ GeV}$ , neglecting the gauge contributions, which are unimportant in this regime, we obtain:

$$\sqrt{m_{\tilde{t}}(m_{\tilde{t}} - \sqrt{\frac{128}{27}}m_t)} \leq m_{\tilde{t}_1} \leq m_{\tilde{t}} \quad , \quad m_{\tilde{t}} \leq m_{\tilde{t}_2} \leq \sqrt{m_{\tilde{t}}(m_{\tilde{t}} + \sqrt{\frac{128}{27}}m_t)} \quad (53)$$

giving indeed a linear behaviour for large  $M_{SUSY}$ :  $M_{SUSY} - \sqrt{\frac{128}{108}}m_t \leq m_{\tilde{t}_1} \leq M_{SUSY}$  and  $M_{SUSY} \leq m_{\tilde{t}_2} \leq M_{SUSY} + \sqrt{\frac{128}{108}}m_t$ .

Finally, we illustrate the impact of the CCB maximal mixing on the CP-even lightest Higgs mass  $m_h$ . At one-loop level, this mass has an upper bound reached for  $\tan \beta = +\infty$ ,  $m_{A^0} \gg m_{Z^0}$ , and the Higgs maximal mixing, eq.(52), [13, 14]. We have shown that the CCB condition rules out such a large stop mixing, therefore this upper bound on  $m_h$  may be lowered <sup>6</sup>. For simplicity, we consider this topic in a simplified setting, somewhat unrealistic, taking only into account leading one-loop contributions coming from top and stops loops. This will already point out the general trend and the importance of CCB condition in this context. In this case, we have [13, 14]

$$m_h^2 \leq m_{Z^0}^2 + \frac{3m_t^4}{4\pi v^2} \left[ \text{Log} \frac{m_t^2}{m_{\tilde{t}}^2} + \frac{A_t}{m_{\tilde{t}}^2} \left( 1 - \frac{A_t}{12m_{\tilde{t}}^2} \right) \right] \quad , \quad v = 174 \text{ GeV} \quad (54)$$

Up to one-loop level, it is consistent to combine the optimal tree-level CCB condition  $A_t \leq A_{t,3}^c$ , eq.(27), illustrated in Fig.4, with this upper bound. Figure 7 illustrates the resulting one-loop CCB bound on  $m_h$  as a function of  $M_{SUSY}$  and compares it with the maximal value reached for the Higgs maximal mixing. As a direct consequence of the aforementioned conservative experimental limit on the lightest stop  $m_{\tilde{t}_1} \gtrsim 100 \text{ GeV}$  [21], three regimes can be considered: i) For  $0 \leq M_{SUSY} \lesssim 310 \text{ GeV}$ , the lightest stop mass experimental bound is more stringent than the CCB maximal mixing. In this regime, we have  $m_h \leq 131 \text{ GeV}$ . The experimental lower bound on  $m_h$  puts in turn lower bounds on  $M_{SUSY}$ . For instance, taking  $m_h \geq 115 \text{ GeV}$ , we must have  $M_{SUSY} \gtrsim 190 \text{ GeV}$ . ii) For  $310 \text{ GeV} \lesssim M_{SUSY} \lesssim 425 \text{ GeV}$ , the CCB maximal mixing becomes more restrictive than the conservative stop experimental bound, while the Higgs maximal mixing is still irrelevant, either because the lightest stop mass is tachyonic or too light. In

---

<sup>6</sup>We note that the CCB maximal mixing, which coincides with the critical bound  $A_{t,3}^c$  in this case, does not depend on the pseudo-scalar mass  $m_{A^0}$ . As will be shown in [11], this interesting property actually extends for all values of  $\tan \beta$  and  $\mu$ .

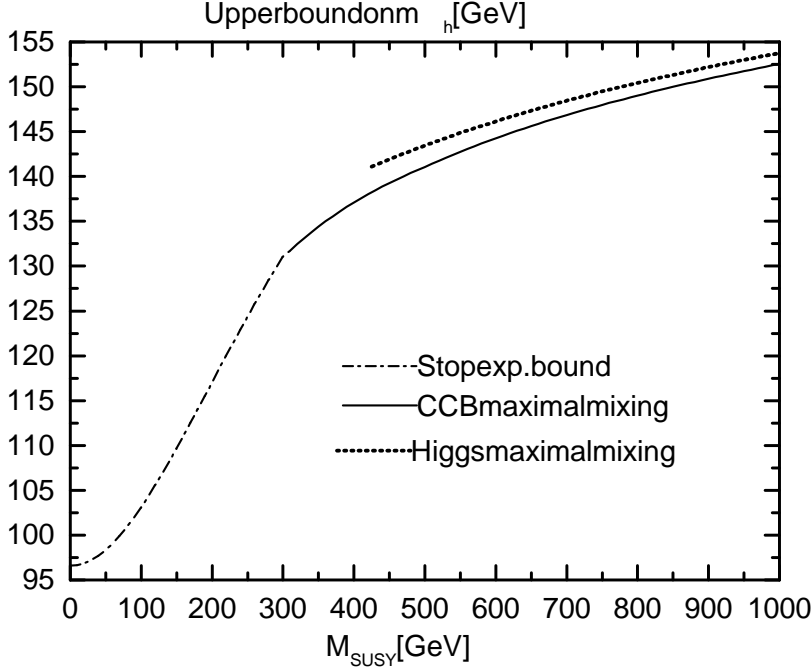


Figure 7: Upper bound on the lightest Higgs mass versus  $M_{SUSY}$ , for  $\tan \beta = +\infty$ . We suppose  $m_{\tilde{t}_1} \gtrsim 100 \text{ GeV}$ . Same set of parameters as in Fig.4.

this regime, eq.(54) combined with the critical CCB condition  $A_{t,3}^c$  [see Figs.4-5] give  $131 \text{ GeV} \leq m_h \leq 138 \text{ GeV}$ . iii) For  $M_{SUSY} \gtrsim 425 \text{ GeV}$ , the CCB and the Higgs maximal mixing are both more restrictive than the experimental bound on the lightest stop. The CCB upper bound on the lightest Higgs is lower than the one for the Higgs maximal-mixing by about  $2.8 \text{ GeV}$  for  $M_{SUSY} \sim 425 \text{ GeV}$ , which is a rather substantial effect. This discrepancy then decreases slowly for larger  $M_{SUSY}$ . We have, e.g., respectively  $\Delta m_h \sim (2.4, 1.5, 1.2) \text{ GeV}$  for  $M_{SUSY} = (500, 750, 1000) \text{ GeV}$ .

A more realistic investigation of the consequences of CCB conditions on  $m_h$  clearly requires that we go beyond the simple approximation given by eq.(54). The complete set of one-loop contributions should be taken into account, including in particular those arising from bottom and sbottoms loops [which are themselves constrained by strong CCB conditions for large  $\tan \beta$ , see Appendix B] [14]. To leading order, we can however trust the discrepancy on the upper bound of the lightest Higgs squared mass between the Higgs and the CCB maximal mixing

$$\Delta m_h^2 = \frac{9(-1 + \eta_{crit}^2)^2 m_t^4}{4\pi^2 v^2}, \quad (55)$$

$\Delta m_h^2$  is actually independent of such additional contributions and depends only of  $M_{SUSY}$  via the critical parameter  $\eta_{crit}$ .

More importantly, two-loop contributions tend to lower substantially this upper bound on the lightest Higgs mass, giving typically  $m_h \lesssim 130 \text{ GeV}$  for  $m_A, M_{susy} \gg m_t$ , with  $\tan \beta \gg 1$  [14]. Two-loop non-logarithmic contributions are also responsible of a slight displacement of the stop mixing value where this upper bound is maximized [14]. A refined study of the importance of CCB conditions in this context, to be consistent at two-loop level, should therefore require a complete one-loop level investigation of CCB



conditions in the plane  $(H_2, \tilde{t}_L, \tilde{t}_R)$ , in order to take also into account sub-leading effects induced by mass discrepancies in the loops. Such a study is clearly beyond the scope of this article and will be the subject of further investigations. We believe however that this simple illustration already clearly indicates the crucial role CCB conditions can play in this phenomenological context.

## 8 Conclusions and outlook

In this article, we have presented at the tree-level a complete model-independent study of the CCB conditions in the plane  $(H_2, \tilde{t}_L, \tilde{t}_R)$ . We have proposed a new procedure to evaluate the CCB VEVs, which moreover enables us to obtain excellent analytical approximations (at the level of the percent) for the VEVs and, ultimately, for the optimal necessary and sufficient conditions on  $A_t$  to avoid CCB. The new conditions incorporate all possible deviations of the CCB vacuum from the D-flat directions, in particular from the  $SU(3)_c$  D-flat direction previously disregarded [5, 6, 7, 8, 9]. We have pointed out that the CCB vacuum typically deviates from the  $SU(3)_c$  D-flat direction and that this feature must be included in a consistent study of CCB conditions to encompass the possibility of avoiding a tachyonic lightest stop. This deviation is controlled essentially by the discrepancy between the soft squark masses  $m_{\tilde{t}_L}, m_{\tilde{t}_R}$ . Rather small in an mSUGRA scenario [where typically  $m_{\tilde{t}_L} \sim m_{\tilde{t}_R}$ ], it can be very large and make substantially more restrictive the critical CCB conditions for  $m_{\tilde{t}_L} \gg m_{\tilde{t}_R}$  or  $m_{\tilde{t}_L} \ll m_{\tilde{t}_R}$ . This should constrain even more model-dependent scenarios, in particular those exhibiting such large mass discrepancies at the SUSY scale, e.g. some anomaly mediated models [4], or, more generally, models incorporating non-universalities for the squark soft masses of the third generation at a high energy scale. In order to take into account one-loop leading corrections, the tree-level CCB conditions obtained in this article should be evaluated at an appropriate scale  $Q \sim Q_{SUSY}$ , where  $Q_{SUSY}$  is an average of the SUSY masses.

In the benchmark scenario,  $M_{SUSY} = m_{\tilde{t}_L} = m_{\tilde{t}_R}$  and  $\tan \beta = +\infty$ , we have illustrated at this scale  $Q_{SUSY}$  some physical consequences of the critical CCB condition in the plane  $(H_2, \tilde{t}_L, \tilde{t}_R)$ . A strong bound on the stop mixing parameter  $\tilde{A}_t$  [ $= A_t$  in this case] was obtained, ruling out by more than 10% the Higgs maximal mixing  $|A_t| = \sqrt{6}m_{\tilde{q}}$ . This led us to introduce a "CCB maximal mixing" for the stop fields. We have exhibited new strong limits on the stop mass spectrum, which simply encode the physical requirement of avoiding CCB. Finally, we have considered the impact of the CCB maximal mixing on the upper bound of the CP-even lightest Higgs in the MSSM,  $m_h$ , at one-loop level, though in a simplified and rather unrealistic setting. Taking into account only top and stop contributions, we have shown that this upper bound can be reduced by up to  $\sim 3$  GeV in comparison with the maximal value reached for the Higgs maximal mixing. We believe that these illustrations stress the importance of a refined study of CCB conditions, such as the one presented here, in the context of Higgs phenomenology. We note however that a more realistic investigation of the upper bound on the lightest Higgs mass,  $m_h$ , requires that we take into account all one-loop contributions to the Higgs mass, not only the leading top and stop ones, but also two-loop contributions. As is well-known, the latter can

be large and also responsible of a displacement of the stop mixing which maximizes  $m_h$  [13, 14]. A refined analysis of this important phenomenological topic, to be consistent at two-loop level, should therefore require a precise one-loop study of CCB conditions in the plane  $(H_2, \tilde{t}_L, \tilde{t}_R)$ , in order to obtain sub-leading contributions that our renormalization group improved tree-level CCB conditions cannot grasp. Such a tedious study will be the subject of future investigations.

In the benchmark scenario considered in this article, we have also pointed out that combining a precise CCB information in the plane  $(H_2, \tilde{t}_L, \tilde{t}_R)$  with a conservative experimental input on the lightest stop mass,  $m_{\tilde{t}_1} \gtrsim 100 \text{ GeV}$ , already indicates that the EW vacuum is the deepest vacuum and is therefore stable in a large part of the parameter space,  $M_{SUSY} \leq 310 \text{ GeV}$ . Similar regions can also be found for any value of  $\tan\beta$  [11]. Outside these regions, following the philosophy of metastability, the EW vacuum can still be considered as safe, even in the presence of a deeper CCB vacuum, provided its lifetime exceeds the age of the Universe [9, 10]. A numerical study of the tunneling rate into the CCB vacuum is required to evaluate the relaxed CCB metastability condition [16]. The present study, which can be straightforwardly completed by giving accurate analytical expressions for the CCB saddle-point, provides also some enlightening pieces of information on the shape of the potential barrier between the vacua, and therefore give essential tools to investigate precisely this feature.

For completeness, it is important to stress that this investigation of CCB condition in the plane  $(H_2, \tilde{t}_L, \tilde{t}_R)$  is also numerically illustrative of what can be found in the extended plane  $(H_1, H_2, \tilde{t}_L, \tilde{t}_R)$ , provided  $\tan\beta \gtrsim 15$  and  $|\mu| \lesssim \text{Min}[m_{A^0}, M_{SUSY}]$ . In particular, the results obtained for the critical CCB bound on  $A_t$  and the physical implications on the stop mixing parameter and the stop mass spectrum are not substantially modified compared to the extreme case  $\tan\beta = +\infty$  illustrated here. In a forthcoming paper, we will present the extension of this study to the plane  $(H_1, H_2, \tilde{t}_L, \tilde{t}_R)$ , and give optimal CCB constraints on  $(A_t, \mu)$  valid for all values of  $\tan\beta$  [11]. We have also re-analyzed in a fully model-independent way the potentially dangerous direction  $(H_1, H_2, \tilde{t}_L, \tilde{t}_R, \tilde{\nu}_L)$ , previously considered in [6]. Additional, though not very restrictive, CCB conditions involving the sneutrino soft mass  $m_{\tilde{\nu}_L}$  will be given [12].

Besides physical implications on the MSSM mass spectrum, the CCB condition on  $A_t$ , completed with one on the  $\mu$  term obtained in the extended plane  $(H_1, H_2, \tilde{t}_L, \tilde{t}_R)$  [11], should also have further important consequences on the phenomenology of the MSSM Higgs bosons [22]. In particular, CCB conditions provide dramatic restrictions on physical processes which require, to be competitive, a stop mixing parameter  $\tilde{A}_t$  as large as the Higgs maximal mixing, e.g., for the production of neutral Higgs bosons associated with top squarks [23]. Further investigations are currently made in this direction in order to delineate more precisely the potential discovery of Supersymmetry.

## Acknowledgement

This work was supported by a Marie Curie Fellowship, under contract No HPMF-CT-1999-00363. I would like to thank especially G.J. Gounaris and P.I. Porfyriadis for their

help and the Theory Group of the University of Thessaloniki for its hospitality. I would like also to thank G. Moulaka for valuable discussions and support during the completion of this work, as well as for reading the manuscript and helping me to improve it. This work was initiated in the French GDR in Supersymmetry. I thank its participants for stimulating discussions. Special thanks also to M. Bezouh.

## Appendix A: The optimal sufficient bound

In this appendix, we give some details on the derivation of the optimal sufficient bound  $A_t^{suf}$  defined in sec.3.3, see eq.(34). Let us consider the extremal equation associated to  $H_2$ , eq.(14):

$$E_{H_2} = \alpha_3 H_2^3 + \beta_3 H_2^2 + \gamma_3 H_2 + \delta_3 = 0 \quad (\text{A.1})$$

where the coefficients  $\alpha_3, \beta_3, \gamma_3, \delta_3$  are given in the text, eqs.(15-18). Obviously,  $\delta_3$  is always positive;  $\beta_3$  is proportional to the positive coefficient of the quadratic term in  $\langle H_2 \rangle$  of  $B_3$ , eq.(6), and is also positive;  $\alpha_3$  is dominated by a large contribution in  $Y_t^4$  and is therefore negative; finally,  $\gamma_3$  is dominated by the negative terms proportional to  $A_t^2$  and  $m_{\tilde{t}_L}^2 + f^2 m_{\tilde{t}_R}^2$  and is negative. The sign of these coefficients imply that any real root of  $E_{H_2}$ , considered as a cubic polynomial in  $H_2$ , must be positive. Moreover, by simple inspection of these roots expressed as a function of the coefficients  $\alpha_3, \beta_3, \gamma_3, \delta_3$ , it is straightforward to show that the necessary and sufficient condition to have only one real root is indeed given by eq.(33).

Let us prove now that the potential  $V_3$ , eq.(1) has no local CCB minimum, if the extremal equation associated to  $H_2$ , eq.(14), has only one real root in  $H_2$  for any value  $f$ .

Equivalently, we can show that if the potential  $V_3$ , eq.(1), has one local CCB minimum ( $\langle H_2 \rangle, \langle \tilde{t}_L \rangle, \langle f \rangle$ ), then for  $f = \langle f \rangle$  the extremal equation  $E_{H_2} = 0$  has necessarily three real roots in  $H_2$ .

Let us consider the following continuous path  $\mathcal{P}$  in the plane  $(H_2, \tilde{t}_L, \tilde{t}_R)$ : for  $\phi \in [0, \tilde{H}_2]$ , we take  $H_2 = \phi, \tilde{t}_L = \tilde{t}_R = 0$ ; for  $\phi \in [\tilde{H}_2, \langle H_2 \rangle]$ , we take  $H_2 = \phi, \tilde{t}_L = \sqrt{-2B_3/A_3}|_{f=\langle f \rangle}, \tilde{t}_R = \langle f \rangle \tilde{t}_L$ , where  $A_3, B_3$  are given in eq.(6). Here, the positive value  $\tilde{H}_2$  denotes the lowest solution of the equation  $B_3 = 0$  for  $f = \langle f \rangle$ . By definition, the path  $\mathcal{P}$  goes through the origin of the fields and also through the local CCB vacuum for  $\phi = \langle H_2 \rangle$  [see eq.(5)].

We can show now that, in this situation, it is absurd to have only one real root for the extremal equation associated to  $H_2$ , eq.(14). By definition, the solutions of this equation provide in particular the value  $H_2$  of any directional extremum in the second part of the path  $\mathcal{P}$ , i.e. for  $\phi \in [\tilde{H}_2, \langle H_2 \rangle]$ . Therefore, assuming that this equation has only one real root for  $f = \langle f \rangle$  implies that on this part of the path  $\mathcal{P}$ , there is no directional saddle-point. What about the first part of the path  $\mathcal{P}$ , i.e. for  $\phi \in [0, \tilde{H}_2]$ ? Here, the potential  $V_3$ , eq.(1), reads:

$$V_3 = H_2^2(m_2^2 + \frac{(g_1^2 + g_2^2)}{8}H_2^2) \quad (\text{A.2})$$

For  $m_2^2 \geq 0$ , this potential is monotonous as a function of  $H_2$  and has no extrema.

Hence, in this case, we finally conclude that we can find a continuous path  $\mathcal{P}$  in the plane  $(H_2, \tilde{t}_L, \tilde{t}_R)$  which connects the origin of the fields and the CCB vacuum, moreover without any directional saddle-point.

We remind the reader that we have assumed in our study positive squared soft mass  $m_{\tilde{t}_L}^2, m_{\tilde{t}_R}^2$  to avoid an obvious CCB problem at the origin of the fields and that the CCB extremum ( $\langle H_2 \rangle, \langle \tilde{t}_L \rangle, \langle f \rangle$ ) we consider is supposed to be a local minimum of the potential  $V_3$ , eq.(1). In this light, the conclusion obtained for  $m_2^2 \geq 0$  is absurd, because in this case the origin of the fields is also a local minimum, so that, necessarily there must be a barrier separating it from the CCB vacuum, and a saddle-point on any path connecting them.

The regime  $m_2^2 \leq 0$  is somewhat more complicated to investigate and requires that we adjust the path  $\mathcal{P}$  to different cases. This comes from the fact that the potential in eq.(A.2) has an additional non-CCB extremum,  $\langle H_2 \rangle_{EW}^2 = -4m_2^2/(g_1^2 + g_2^2)$ , as noted see sec.3.4. Therefore, the cases  $\langle H_2 \rangle \ll \langle H_2 \rangle_{EW}$ ,  $\langle H_2 \rangle \sim \langle H_2 \rangle_{EW}$ , and  $\langle H_2 \rangle \gg \langle H_2 \rangle_{EW}$  should be considered separately. The path  $\mathcal{P}$  proposed is obviously only adapted to the last case. We will not enter into such a detailed, but straightforward, demonstration. Actually, assuming that this additional non-CCB extremum is a local minimum, as done in this article [see sec.3.4, eq.(39)], it is easy to convince one-self that in all these cases a conclusion similar to the one obtained for  $m_2^2 \geq 0$  is obtained: it is absurd to suppose that the extremal equation associated to  $H_2$ , eq.(14), has only one solution in  $H_2$  for  $f = \langle f \rangle$ , because on any path connecting this additional non-CCB minimum and the CCB minimum, there should be a saddle-point which necessarily would show as an additional real solution of this equation.

Hence, without loss of generality, we conclude that if  $E_{H_2} = 0$  has only one real solution in  $H_2$  for any value of  $f$ , then the potential  $V_3$ , eq.(1), cannot have any local CCB minimum. In such a situation, the unique solution of  $E_{H_2} = 0$  found is spurious and located outside the compact domain where  $\langle \tilde{t}_L \rangle^2 \geq 0$ , eqs.(12,13).

## Appendix B: CCB conditions in the plane $(H_1, \tilde{b}_L, \tilde{b}_R)$

The procedure to evaluate the VEVs of the extrema of the potential and the geometrical picture presented in this article hold also for the tree-level potential in the plane  $(H_1, \tilde{b}_L, \tilde{b}_R)$ , provided the bottom Yukawa coupling  $Y_b$  is large enough, or equivalently for large  $\tan \beta$ . Here,  $\tilde{b}_L$  and  $\tilde{b}_R$  stand for the left and right sbottom fields of the same generation, and  $H_1$  is the neutral component of the corresponding Higgs  $SU(2)_L$  scalar doublet. In this plane, the tree-level potential reads [1, 5]:

$$\begin{aligned} \bar{V}_3 = & m_1^2 H_1^2 + m_{\tilde{b}_L}^2 \tilde{b}_L^2 + m_{\tilde{b}_R}^2 \tilde{b}_R^2 - 2Y_b A_b H_1 \tilde{b}_L \tilde{b}_R + Y_b^2 (H_1^2 \tilde{b}_L^2 + H_1^2 \tilde{b}_R^2 + \tilde{b}_L^2 \tilde{b}_R^2) \\ & + \frac{g_1^2}{8} (H_1^2 - \frac{\tilde{b}_L^2}{3} - \frac{2\tilde{b}_R^2}{3})^2 + \frac{g_2^2}{8} (H_1^2 - \tilde{b}_L^2)^2 + \frac{g_3^2}{6} (\tilde{b}_L^2 - \tilde{b}_R^2)^2 \end{aligned} \quad (\text{B.1})$$

This potential is similar to  $V_3$ , eq.(1). In fact, redefining the fields and parameters of  $\bar{V}_3$  as follows [1, 5, 6]

$$H_1 \rightarrow H_2 \quad , \quad \tilde{b}_{R/L} \rightarrow \tilde{u}_{R/L}$$

$$m_1 \rightarrow m_2 \quad , \quad m_{\tilde{b}_{R/L}} \rightarrow m_{\tilde{u}_{R/L}} \quad , \quad Y_b \rightarrow Y_u \quad (\text{B.2})$$

we recover  $V_3$ , eq.(1), except for a minor difference coming from the  $U(1)_Y$  D-term. The relevant expressions to study CCB conditions in this plane are the following ones. The VEV  $\langle \tilde{b}_L \rangle$  verifies:

$$\bar{A}_3 \langle \tilde{b}_L \rangle^2 + 2\bar{B}_3 = 0 \quad (\text{B.3})$$

where

$$\bar{A}_3 \equiv g_1^2(2 \langle f_b \rangle^2 + 1)^2/18 + g_2^2/2 + 2g_3^2(\langle f_b \rangle^2 - 1)^2/3 + 4Y_b^2 \langle f_b \rangle^2 \quad (\text{B.4})$$

$$\begin{aligned} \bar{B}_3 \equiv & \langle H_1 \rangle^2 \frac{[12Y_b^2(\langle f_b \rangle^2 + 1) - 3g_2^2 - g_1^2(2 \langle f_b \rangle^2 + 1)]}{12} \\ & - 2A_b Y_b \langle f_b \rangle \langle H_1 \rangle + m_{\tilde{b}_L}^2 + \langle f_b \rangle^2 m_{\tilde{b}_R}^2 \end{aligned} \quad (\text{B.5})$$

with  $f_b \equiv \tilde{b}_L/\tilde{b}_R$ . Quite similarly to what happens in the plane  $(H_2, \tilde{t}_L, \tilde{t}_R)$ ,  $\bar{B}_3$  tells us when the large bottom Yukawa regime opens. This occurs, whatever  $\langle f_b \rangle$ , for  $Y_b \geq \text{Max}[\sqrt{(g_1^2 + 3g_2^2)/12}, g_1/\sqrt{6}] \sim 0.3$  (at the EW scale). Using the tree-level relation  $m_t/m_b = Y_t/Y_b \tan \beta \sim 35$  [1], with  $Y_t \sim 1$ , this requires  $\tan \beta \gtrsim 10.5$ .

In this large  $\tan \beta$  regime, we obtain a sufficient bound to avoid CCB in the plane  $(H_1, \tilde{b}_L, \tilde{b}_R)$ , similar to  $A_t^{(0)}$ , eq.(9). It reads

$$A_b \leq A_b^{(0)} \equiv m_{\tilde{b}_L} \sqrt{1 - \frac{g_1^2}{6Y_b^2}} + m_{\tilde{b}_R} \sqrt{1 - \frac{(3g_2^2 + g_1^2)}{12Y_b^2}} \quad (\text{B.6})$$

We note however that  $A_b^{(0)}$  can be quite small for  $Y_b \sim \sqrt{(g_1^2 + 3g_2^2)/12}$ .

The extremal equation associated to  $\langle H_1 \rangle$  reads

$$\bar{\alpha}_3 H_1^3 + \bar{\beta}_3 H_1^2 + \bar{\gamma}_3 H_1 + \bar{\delta}_3 = 0 \quad (\text{B.7})$$

with

$$\begin{aligned} \bar{\alpha}_3 = & -36Y_b^4(f_b^2 + 1)^2 + [3g_3^2(g_1^2 + g_2^2) + g_1^2 g_2^2](f_b^2 - 1)^2 \\ & + 6Y_b^2 g_1^2(2f_b^4 + 6f_b^2 + 1) + 18Y_b^2 g_2^2(2f_b^2 + 1) \end{aligned} \quad (\text{B.8})$$

$$\bar{\beta}_3 = 9A_b Y_b f_b [12(f_b^2 + 1)Y_b^2 - (2f_b^2 + 1)g_1^2 - 3g_2^2] \quad (\text{B.9})$$

$$\begin{aligned} \bar{\gamma}_3 = & -72A_b^2 f_b^2 Y_b^2 - 3(m_{\tilde{b}_L}^2 + f_b^2 m_{\tilde{b}_R}^2)[12Y_b^2(f_b^2 + 1) - g_1^2(2f_b^2 + 1) - 3g_2^2] \\ & + m_1^2 [72Y_b^2 f_b^2 + g_1^2(2f_b^2 + 1)^2 + 9g_2^2 + 12g_3^2(f_b^2 - 1)^2] \end{aligned} \quad (\text{B.10})$$

$$\bar{\delta}_3 = 36A_b Y_b f_b (m_{\tilde{b}_L}^2 + f_b^2 m_{\tilde{b}_R}^2) \quad (\text{B.11})$$

The extremal equation associated to  $f_b$  reads

$$\bar{a}_3 f_b H_1^2 + \bar{b}_3 H_1 + \bar{c}_3 f_b = 0 \quad (\text{B.12})$$

with

$$\begin{aligned} \bar{a}_3 = & 2Y_b^2[(18Y_b^2 - 12g_3^2)(f_b^2 - 1) + 9g_2^2 - g_1^2(4f_b^2 - 1)] \\ & + (f_b^2 - 1)[g_1^2 g_2^2 + 3(g_1^2 + g_2^2)g_3^2] \end{aligned} \quad (\text{B.13})$$

$$\bar{b}_3 = A_b Y_b [12g_3^2(f_b^4 - 1) - 9g_2^2 + g_1^2(4f_b^4 - 1)] \quad (\text{B.14})$$

$$\begin{aligned} \bar{c}_3 = & -m_{\tilde{b}_L}^2 [36Y_b^2 + 12g_3^2(f_b^2 - 1) + 2g_1^2(2f_b^2 + 1)] \\ & + m_{\tilde{b}_R}^2 [36f_b^2 Y_b^2 - 12g_3^2(f_b^2 - 1) + 9g_2^2 + g_1^2(2f_b^2 + 1)] \end{aligned} \quad (\text{B.15})$$

The VEVs ( $\langle H_1 \rangle, \langle f_b \rangle$ ) of a consistent CCB vacuum has to verify this set of coupled equations and must furthermore be included in the compact domain where  $\langle \tilde{b}_L \rangle^2 \geq 0$ . The recursive algorithm to compute the VEVs of the CCB vacuum is identical to the one presented in the text for the top Yukawa coupling regime. A convenient initial value to accelerate the procedure is  $f_{b,3}^{(0)} = \sqrt{\frac{A_b^2 + 2m_{\tilde{b}_L}^2 - m_{\tilde{b}_R}^2}{A_b^2 + 2m_{\tilde{b}_R}^2 - m_{\tilde{b}_L}^2}}$ .

The optimal sufficient bound on  $A_b^{suf}$  below which no CCB vacuum may develop in the plane  $(H_1, \tilde{b}_L, \tilde{b}_R)$  is always given by the largest solution in  $A_b$  of the equation  $\bar{\mathcal{C}}_3 \equiv [\bar{\beta}_3^3 - 9\bar{\alpha}_3\bar{\beta}_3\bar{\gamma}_3 + 27\bar{\alpha}_3^2\bar{\delta}_3]^2 + 4[-\bar{\beta}_3^2 + 3\bar{\alpha}_3\bar{\gamma}_3]^3 = 0$ , taking  $f = f_{b,3}^{(0)}$ .

The potential  $\bar{V}_3$ , eq.(B.1), can have at most three extrema: the origin of the fields, a CCB local minimum and a CCB saddle-point. In particular, there is no additional non-CCB extremum. Such a possibility would appear for  $m_1^2 \leq 0$ , which requires  $\tan \beta \sim 0$ . This is obviously outside the large bottom Yukawa coupling regime and is, moreover, ruled out by experimental data. Finally, the necessary and sufficient bound  $A_{b,3}^c$  is obtained by scanning the region  $A_b \geq A_b^{suf}$  and comparing the potential  $\bar{V}_3$  with the EW potential  $\langle V \rangle|_{EW}$ , eq.(26). For large  $\tan \beta$ , which implies  $Y_b \sim 1$ , the appropriate renormalization scale to evaluate the tree-level CCB conditions  $A_b^{suf}, A_{b,3}^c$  in order to incorporate one-loop leading corrections, is the SUSY scale  $Q_{SUSY}$ , quite similarly to the case  $(H_2, \tilde{t}_L, \tilde{t}_R)$ .

## References

- [1] See for instance, P. Fayet, S. Ferrara, Phys. Rep. 32 (1977) 249; H.P. Nilles, Phys. Rep. 110 (1984) 1; H.E. Haber, G.L. Kane, Phys. Rep. 117 (1985) 75; A.B. Lahanas, D.V. Nanopoulos, Phys. Rep. 145 (1987) 1; R. Arnowitt, P. Nath, Report CPT-TAMU-52-93; M. Drees, S. Martin, hep-ph/9504324; S. Martin, hep-ph/9709356
- [2] J. Wess, J. Bagger, Supersymmetry and Supergravity, Princeton Series in Physics
- [3] For the mSUGRA scenario: A.H. Chamseddine, R. Arnowitt, P. Nath, Phys. Lett. 49 (1982) 970; R. Barbieri, S. Ferrara, C.A. Savoy, Phys. Lett. **B119** (1982) 343; L. Hall, J. Lykken, S. Weinberg, Phys. Rev. **D 27** (1983) 2359; For the Gauge Mediated scenario: M. Dine, W. Fischler, M. Srednicki, Nucl. Phys. **B189**(1981) 575; S. Dimopoulos, S. Raby, Nucl. Phys. **B192** (1981) 353; G.F. Giudice, R. Rattazzi, Phys. Rept. **322** (1999) 419, 501
- [4] for the Anomaly Mediated scenario, see for instance L. Randall, R. Sundrum, Nucl. Phys. **B557** (1999) 79; G.F. Giudice, M. Luty, H. Murayama, R. Rattazzi, JHEP 9812 (1998) 27; see also P. Binetruy, M.K. Gaillard, B. Nelson, hep-ph/0011081
- [5] J.M. Frere, D.R.T. Jones, S. Raby, Nucl. Phys. **B222** (1983) 11; L. Alvarez-Gaumé, J. Polchinski, M. Wise, Nucl. Phys. **B221** (1983) 495; M. Claudson, L.J. Hall, I. Hintchcliffe, Nucl. Phys. **B228** (1983) 501; H.P. Nilles, M. Srednicki, D. Wyler, Phys. Lett. **B120** (1983) 346; J.P. Derendiger, C.A. Savoy, Nucl. Phys. **B237** (1984) 307; C. Kounas, A.B. Lahanas, D.V. Nanopoulos, M. Quirós, Nucl. Phys. **B236** (1984)

- 438; M. Drees, M. Glück, K. Grassie, Phys. Lett. **B157** (1995) 164; J.F. Gunion, H.E. Haber, M. Sher, Nucl. Phys. **B306** (1988) 1; H. Komatsu, Phys. Lett. **B215** (1988) 323
- [6] J.A. Casas, A. Lleyda, C. Muñoz, Nucl. Phys. **B471** (1995)3
- [7] J.A. Casas, S. Dimopoulos, Phys. Lett. **B387** (1996) 107; J.A. Casas, A. Lleyda, C. Muñoz, Phys. Lett. **B389** (1996) 305; H. Baer, M. Brhlik, D. Castaño, Phys. Rev. **D54** (1996) 6944; J.A. Casas, hep-ph/9707475; S.A. Abel, C.A. Savoy, Nucl. Phys. **B532** (1998) 3; S.A. Abel, C.A. Savoy, Phys. Lett. **B444** (1998) 119; S.A. Abel, T. Falk, Phys. Lett. **B444** (1998) 427; J.A. Casas, A. Ibarra, C. Muñoz, Nucl. Phys. **B554** (1999) 67; A. Dedes, A.E. Farragi, Phys. Rev. **D62** (2000) 016010 ; S.A. Abel, B.C. Allanach, hep-ph/9909448
- [8] A. Bordner, hep-ph/9506409
- [9] P.Langaker, N. Polonski, Phys. Rev. **D50** (1994) 2199; A. Riotto, E. Roulet, Phys. Lett. **B377** (1996) 60; A. Strumia, Nucl. Phys. **B482** (1996) 24; T. Falk, K.A. Olive, L. Roszkowski, M. Sredniki, Phys. Lett. **B367** (1996) 183; A. Kusenko, P. Langaker, G. Segré, Phys. Rev. **D54** (1996) 5824; T. Falk, K.A. Olive, L. Roszkowski, A. Singh, M. Sredniki, Phys. Lett. **B396** (1997) 50; L. Dasgupta, R. Rademacher, P. Suranyi, Phys. Lett. **B447** (1999) 284
- [10] A. Kusenko, P. Langaker, G. Segré, Phys. Rev. **D54** (1996) 5824
- [11] C. Le Mouél, in preparation
- [12] C. Le Mouél, G. Moulataka, in preparation
- [13] H.E. Haber, R. Hempfling, Phys. Rev. Lett **66** (1991) 1815; Y. Okada, M. Yamaguchi, T. Yanagida, Prog. Theor. Ohys. **85** (1991)1; J. Ellis, G. Ridolfi, F. Zwirner, Phys. Lett. **B257** (1991) 83 and **B262** (1991) 477; R. Barbieri, M. Frigeni, Phys. Lett. **B258** (1991) 395
- [14] See for instance M. Carena, M. Carena, H.E. Haber, S. Heinemeyer, W. Hollik, C.E.M. Wagner, G. Weiglein, Nucl. Phys. **B580** (2000) 29 and references therein
- [15] G. Gamberini, G. Ridolfi, F. Zwirner, Nucl.Phys. **B331** (1990) 331; B. de Carlos and J.A. Casas, Phys. Lett. **B309** (1993) 320
- [16] S. Coleman, Phys. Rev. **D15** (1977) 2929; C.G. Callan, S. Coleman, Phys. Rev. **D16** (1977) 1762; A. Kusenko. Phys. Lett. **B377** (1996) 245; I. Dasgupta, Phys. Lett. **B394** (1997) 16
- [17] C.T. Hill, Phys. Rev. **D24** (1981) 691; C.T. Hill, C.N. Leung, S. Rao, Nucl. Phys **B262** (1985) 517; M. Carena, M. Olechowski, S. Pokorski, C.E.M. Wagner, Nucl. Phys. **B419** (1994) 217; M. Carena, C.E.M. Wagner, Nucl. Phys. **B452** (1995) 45; M. Lanzaagorta, G. Ross, Phys. Lett. **B364** (1995) 163; M. Carena, P. Chankowski, M. Olechowski, S. Pokorski, C.E.M. Wagner, Nucl. Phys. **B491** (1997) 103;

- [18] D.I. Kazakov, G. Moultaka, Nucl. Phys. **B577** (2000) 121; G.K. Yeghiyan, M. Jurcisin, D.I. Kazakov, Mod. Phys. Let. **A14** (1999) 601; M. Jurcisin, D.I. Kazakov, Mod. Phys. Let. **A14** (1999) 671
- [19] D.J. Castaño, E.J. Piard, P. Ramond, Phys. Rev. **D49** (1994) 4882; M. Carena et al, Nucl. Phys. **B426** (1994) 269; W. De Boer, R. Ehret, D.I. Kazakov, Z. Phys. **C67** (1994) 647; V. Barger, M.S. Berger, P. Ohmann, Phys. Rev. **D49** (1994) 4908; M. Drees, S. Martin, hep-ph/9504324
- [20] M. Bando, T. Kugo, N. Maekawa, H. Nakano, Phys. Lett. **B301** (1993) 83; see also C. Ford, D.R.T. Jones, P.W. Stephenson, M.B. Einhorn Nucl. Phys. **B395** (1993) 17; M. Bando, T. Kugo, N. Maekawa, H. Nakano, Prog.Theor.Phys. 90 (1993) 405; C. Ford and C. Wiesendanger, Phys. Lett. **B398** (1997) 342 and Phys. Rev. **D55** (1997) 2202; J.A. Casas, V. Di Clemente and M. Quirós, Nucl. Phys. **B553** (1999) 511
- [21] CDF Collaboration, Abstract 652, Conference ICHEP 98, July 1998; OPAL Collaboration, G. Abiendi et al., Phys. Lett. **B456** (1999) 95
- [22] For a recent reviews, see for instance A. Djouadi, R. Kinnunen, E. Richter Was, H.U. Martyn et al., hep-ph/0002258 and M. Carena, J.S. Conway, H. E. Haber, J.D. Hobs et al., hep-ph/00010338 and references therein
- [23] See A. Djouadi, J.L. Kneur, G. Moultaka, Nucl. Phys. **B569** (2000) 53 and references therein